# Cambrian triangulations and their tropical realizations

Vincent Pilaud

# CAMBRIAN TRIANGULATIONS AND THEIR TROPICAL REALIZATIONS

VINCENT PILAUD

Abstract. This paper develops a Cambrian extension of the work of C. Ceballos, A. Padrol and C. Sarmiento on $\nu$-Tamari lattices and their tropical realizations. For any signature $\varepsilon \in \{\pm\}^n$, we consider a family of $\varepsilon$-trees in bijection with the triangulations of the $\varepsilon$-polygon. These $\varepsilon$-trees define a flag regular triangulation $\mathcal{T}^\varepsilon$ of the subpolytope $\operatorname{conv}\{(\mathbf{e}_{i_\bullet}, \mathbf{e}_{j_\circ}) \mid 0 \le i_\bullet < j_\circ \le n+1\}$ of the product of simplices $\triangle_{\{0_\bullet,\dots,n_\bullet\}} \times \triangle_{\{1_\circ,\dots,(n+1)_\circ\}}$. The oriented dual graph of the triangulation $\mathcal{T}^\varepsilon$ is the Hasse diagram of the (type $A$) $\varepsilon$-Cambrian lattice of N. Reading. For any $I_\bullet \subseteq \{0_\bullet,\dots,n_\bullet\}$ and $J_\circ \subseteq \{1_\circ,\dots,(n+1)_\circ\}$, we consider the restriction $\mathcal{T}^\varepsilon_{I_\bullet,J_\circ}$ of the triangulation $\mathcal{T}^\varepsilon$ to the face $\triangle_{I_\bullet} \times \triangle_{J_\circ}$. Its dual graph is naturally interpreted as the increasing flip graph on certain $(\varepsilon, I_\bullet, J_\circ)$-trees, which is shown to be a lattice generalizing in particular the $\nu$-Tamari lattices in the Cambrian setting. Finally, we present an alternative geometric realization of $\mathcal{T}^\varepsilon_{I_\bullet,J_\circ}$ as a polyhedral complex induced by a tropical hyperplane arrangement.

## 1. Introduction

The Tamari lattice is a fundamental structure on Catalan objects such as triangulations of a convex polygon, binary trees, or Dyck paths. It is defined as the reflexive and transitive closure of the graph of slope increasing flips on triangulations, of right rotations on binary trees, or of subpath translations on Dyck paths. Introduced by D. Tamari in [Tam51], it has been largely studied and extended in several directions, see [MHPS12] and the references therein for surveys on its various connections. Two particularly relevant generalizations of the Tamari lattice are needed for the purposes of this paper.

On the one hand, N. Reading [Rea06] observed that, although the graph of flips between triangulations does not depend on the positions of the vertices of the convex polygon, the orientation of the flip graph does. The different orientations can be encoded combinatorially by a signature $\varepsilon \in \{\pm\}^n$. This signature defines a $\varepsilon$-polygon, and the graph of slope increasing flips between triangulations of this $\varepsilon$-polygon gives the $\varepsilon$-Cambrian lattice. This generalization has been essential in further combinatorial, geometric and algebraic developments of Coxeter Catalan combinatorics, in particular:

(i) it underlined the importance of lattice congruences of the weak order and brought lattice theoretic tools to the development of Catalan combinatorics [Rea04, Rea16b, Rea16a],
(ii) it opened the door to the study of Cambrian lattices [Rea06] for arbitrary finite Coxeter groups, in connection to the theory of finite type cluster algebras of S. Fomin and A. Zelevinsky [FZ02, FZ03],
(iii) it was essential for the construction of associahedra, cyclohedra and generalized associahedra by C. Hohlweg, C. Lange and H. Thomas [HL07, HLT11],
(iv) it paved the ground to the construction of Cambrian and permutree Hopf algebras [CP17, PP18], providing unified descriptions of the classical Hopf algebras of C. Malvenuto and C. Reutenauer on permutations [MR95] and J.-L. Loday and M. Ronco on binary trees [LR98].

On the other hand, L.-F. Préville-Ratelle and X. Viennot introduced $\nu$-Tamari lattices in [PRV17]. The $\nu$-Tamari lattice is a lattice structure on all Dyck paths that are located above a given Dyck path $\nu$. As it turns out, the classical Tamari lattice is partitioned by smaller $\nu$-Tamari lattices corresponding to the different possible canopies of the binary trees [PRV17]. The $\nu$-Tamari lattices also exhibit various combinatorial, geometric and algebraic connections:

Partially supported by the French ANR grants SC3A (15 CE40 0004 01) and CAPPS (17 CE40 0018), and by the project "Austria/France Scientific & Technological Cooperation" (BMWFW Project No. FR 10/2018 and PHC Amadeus 2018 Project No. 39444WJ).

(i) they were introduced with motivations coming from rational Catalan combinatorics in connection to combinatorial interpretations of dimension formulas in trivariate and higher multivariate diagonal harmonics [Ber13, BPR12],
(ii) their intervals are enumerated by simple formulas also counting non-separable planar maps [Cha07, BB09, BMFPR11, FPR17],
(iii) they correspond to certain face restrictions of a classical triangulation of a product of two simplices [CPS18], and therefore admit realizations as polyhedral complexes defined by tropical hyperplane arrangements, as will be described in details below,
(iv) they play an essential role in the Hopf algebra on pipe dreams recently developed in [BCP18].

The objectives of this paper are to explore connections between (type $A$) Cambrian lattices and $\nu$-Tamari lattices, and to define a relevant notion of $\nu$-Cambrian lattices with potential geometric and algebraic connections. One possible approach would be to define $\nu$-Cambrian lattices as the intervals of the Cambrian lattices corresponding to the Cambrian trees with canopy encoded by the path $\nu$. This perspective defines interesting lattices and even extends to arbitrary finite Coxeter groups, but it completely overpasses the geometric interpretation of C. Ceballos, A. Padrol and C. Sarmiento [CPS18] in terms of triangulations of products of simplices and tropical hyperplane arrangements. Instead, we extend the work of [CPS18] to define $\nu$-Cambrian lattices as increasing flip graphs of certain bipartite trees corresponding to certain face restrictions of a certain triangulation of a product of simplices.

To be more precise, let us briefly review the construction of [CPS18] which provides the prototype of our construction. It starts from a family of non-crossing alternating trees in bijection with the triangulations of the $(n+2)$-gon. These trees define a flag regular triangulation $\mathcal{T}$ of the subpolytope $U := \operatorname{conv}\{(\mathbf{e}_{i_\bullet}, \mathbf{e}_{j_\circ}) \mid 0 \le i_\bullet < j_\circ \le n+1\}$ of the product of simplices $\triangle_{\{0_\bullet,\dots,n_\bullet\}} \times \triangle_{\{1_\circ,\dots,(n+1)_\circ\}}$. The dual graph of this triangulation $\mathcal{T}$ is the Hasse diagram of the Tamari lattice. Note that this interpretation of the Tamari lattice as the dual graph of the non-crossing triangulation is ubiquitous in the literature as discussed in [CPS18, Sect. 1.4]. For any subsets $I_\bullet \subseteq \{0_\bullet, \dots, n_\bullet\}$ and $J_\circ \subseteq \{1_\circ, \dots, (n+1)_\circ\}$, they consider the restriction $\mathcal{T}_{I_\bullet,J_\circ}$ of the triangulation $\mathcal{T}$ to the face $\triangle_{I_\bullet} \times \triangle_{J_\circ}$. The simplices of $\mathcal{T}_{I_\bullet,J_\circ}$ correspond to certain non-crossing alternating $(I_\bullet, J_\circ)$-trees which are in bijection with Dyck paths above a fixed path $\nu(I_\bullet, J_\circ)$. Moreover, the dual graph of $\mathcal{T}_{I_\bullet,J_\circ}$ is the flip graph on $(I_\bullet, J_\circ)$-trees, isomorphic to the Hasse diagram of the $\nu(I_\bullet, J_\circ)$-Tamari poset of [PRV17]. This poset actually embeds as an interval of the classical Tamari lattice and is therefore itself a lattice. This interpretation provides three geometric realizations of the $\nu(I_\bullet, J_\circ)$-Tamari lattice [CPS18, Thm. 1.1]: as the dual of the regular triangulation $\mathcal{T}_{I_\bullet,J_\circ}$, as the dual of a coherent mixed subdivision of a generalized permutahedron, and as the edge graph of a polyhedral complex induced by a tropical hyperplane arrangement.

In this paper, we extend this approach in the (type $A$) Cambrian setting. For any signature $\varepsilon \in \{\pm\}^n$, we consider a family of $\varepsilon$-trees in bijection with the triangulations of the $\varepsilon$-polygon. These $\varepsilon$-trees define a flag regular triangulation $\mathcal{T}^\varepsilon$ of $U$ whose dual graph is the Hasse diagram of the (type $A$) $\varepsilon$-Cambrian lattice of N. Reading [Rea06]. We thus call this triangulation $\mathcal{T}^\varepsilon$ the $\varepsilon$-Cambrian triangulation of $U$. In contrast to the classical Tamari case (obtained when $\varepsilon = -^n$), we are not aware that this triangulation of $U$ was considered earlier in the literature and the proof of its regularity is a little more subtle in the Cambrian case. For any $I_\bullet \subseteq \{0_\bullet, \dots, n_\bullet\}$ and $J_\circ \subseteq \{1_\circ, \dots, (n+1)_\circ\}$, we then consider the restriction $\mathcal{T}^\varepsilon_{I_\bullet,J_\circ}$ of the triangulation $\mathcal{T}^\varepsilon$ to the face $\triangle_{I_\bullet} \times \triangle_{J_\circ}$. Its simplices correspond to certain $(\varepsilon, I_\bullet, J_\circ)$-trees and its dual graph is the increasing flip graph on these $(\varepsilon, I_\bullet, J_\circ)$-trees. Our main combinatorial result is that this increasing flip graph is still an interval of the $\varepsilon$-Cambrian lattice in general. The proof is however more involved than in the classical case ($\varepsilon = -^n$) since this interval does not anymore correspond to a canopy class in general. Finally, we mimic the method of [CPS18, Sect. 5] to obtain an alternative geometric realization of $\mathcal{T}^\varepsilon_{I_\bullet,J_\circ}$ as a polyhedral complex induced by a tropical hyperplane arrangement. We finally note that we only consider here the type $A$ Cambrian lattices, and we leave open the problem to extend our approach to the type $B$ Cambrian lattices. This could probably be treated similarly as was already observed for the classical type $B$ Tamari lattice in [CPS18].

## 2. $(\varepsilon, I_\bullet, J_\circ)$-TREES AND THE $(\varepsilon, I_\bullet, J_\circ)$-COMPLEX

This section defines two polygons and certain families of trees associated to a signature $\varepsilon \in \{\pm\}^n$.

2.1. **Two $\varepsilon$-polygons.** We consider three decorated copies of the natural numbers: the squares $\mathbb{N}_\square$, the blacks $\mathbb{N}_\bullet$ and the whites $\mathbb{N}_\circ$. For $n \in \mathbb{N}$, we use the standard notation $[n] := \{1, \dots, n\}$ and define $[\![n]\!] := \{0, \dots, n\}$, $[n] := \{1, \dots, n+1\}$ and $[\![n]\!] := \{0, \dots, n+1\}$. We write $[n_\square]$, $[n_\bullet]$, $[n_\circ]$ and so on for the decorated versions of these intervals. Fix a signature $\varepsilon \in \{\pm\}^n$. We consider two convex polygons associated to the signature $\varepsilon$ as follows:

- a $(n+2)$-gon $\mathrm{P}^\varepsilon_\square$ with square vertices labeled by $[\![n_\square]\!]$ from left to right and where vertex $i_\square$ is above the segment $(0_\square, (n+1)_\square)$ if $\varepsilon_i = +$ and below it if $\varepsilon_i = -$.
- a $(2n+2)$-gon $\mathrm{P}^\varepsilon_{\bullet\circ}$ with black or white vertices, obtained from $\mathrm{P}^\varepsilon_\square$ by replacing the square vertex $0_\square$ (resp. $(n+1)_\square$) by the black vertex $0_\bullet$ (resp. white vertex $(n+1)_\circ$), and splitting each other square vertex $i_\square$ into a pair of white and black vertices $i_\circ$ and $i_\bullet$ (such that the vertices of $\mathrm{P}^\varepsilon_{\bullet\circ}$ are alternatively colored black and white). The black (resp. white) vertices of $\mathrm{P}^\varepsilon_{\bullet\circ}$ are labeled by $[\![n_\bullet]\!]$ (resp. $[n_\circ]$) from left to right. We will only consider diagonals of the form $(i_\bullet, j_\circ)$ with $i_\bullet < j_\circ$, so that we do not draw the edges $(i_\circ, i_\bullet)$ of this $\varepsilon$-polygon.

Examples of these polygons are represented in Figure 1 for the signature $\varepsilon = -++-+--+$.

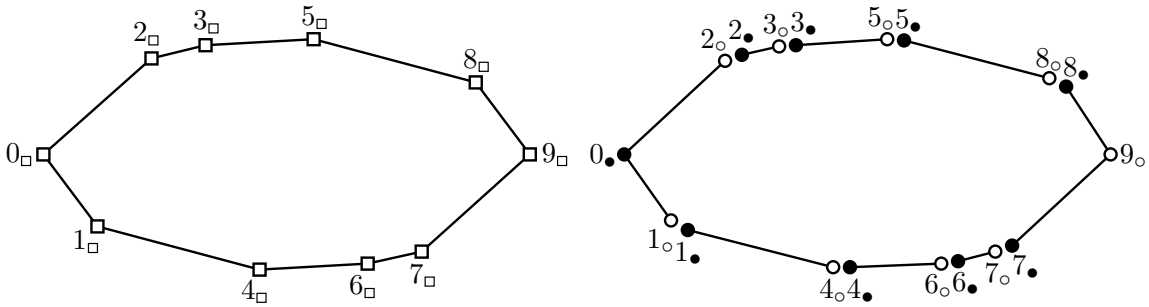


FIGURE 1. The polygons $\mathrm{P}^\varepsilon_\square$ (left) and $\mathrm{P}^\varepsilon_{\bullet\circ}$ (right) for the signature $\varepsilon = -++-+--+$.

2.2. **$(\varepsilon, I_\bullet, J_\circ)$-trees.** All throughout the paper, we consider $I_\bullet \subseteq [\![n_\bullet]\!]$ and $J_\circ \subseteq [n_\circ]$ and we always assume that $\min(I_\bullet) < \min(J_\circ)$ and $\max(I_\bullet) < \max(J_\circ)$. Consider the graph $\mathrm{G}^\varepsilon_{I_\bullet, J_\circ}$ with vertices $I_\bullet \cup J_\circ$ and edges $\{(i_\bullet, j_\circ) \mid i_\bullet \in I_\bullet,\, j_\circ \in J_\circ,\, i_\bullet < j_\circ\}$. Note that this graph is geometric: its vertices are considered as vertices of $\mathrm{P}^\varepsilon_{\bullet\circ}$ and its edges are considered as straight edges in $\mathrm{P}^\varepsilon_{\bullet\circ}$. A subgraph of $\mathrm{G}^\varepsilon_{I_\bullet, J_\circ}$ is *non-crossing* if no two of its edges cross in their interior.

**Proposition 1.** *Any maximal non-crossing subgraph of $\mathrm{G}^\varepsilon_{I_\bullet, J_\circ}$ is a spanning tree of $\mathrm{G}^\varepsilon_{I_\bullet, J_\circ}$.*

*Proof.* The proof works by induction on $|I_\bullet| + |J_\circ|$. The result is immediate when $|I_\bullet| = |J_\circ| = 1$. Assume now for instance that $|I_\bullet| > 1$ (the case $|I_\bullet| = 1$ and $|J_\circ| > 1$ is similar). Let $i_\bullet := \max(I_\bullet)$ and $j_\circ := \min\big(\{j_\circ \in J_\circ \mid i_\bullet < j_\circ \text{ and } \varepsilon_i = \varepsilon_j\} \cup \{\max(J_\circ)\}\big)$. Note that our choice of $j_\circ$ ensures that $(i_\bullet, j_\circ)$ is a boundary edge of $\mathrm{conv}(I_\bullet \cup J_\circ)$. Moreover, any edge of $\mathrm{G}^\varepsilon_{I_\bullet, J_\circ}$ incident to $i_\bullet$ is of the form $(i_\bullet, j'_\circ)$ for $i_\bullet < j'_\circ$ while any edge of $\mathrm{G}^\varepsilon_{I_\bullet, J_\circ}$ incident to $j_\circ$ is of the form $(i'_\bullet, j_\circ)$ for $i'_\bullet \le i_\bullet$ (by maximality of $i_\bullet$). Therefore, all edges of $\mathrm{G}^\varepsilon_{I_\bullet, J_\circ} \smallsetminus \{(i_\bullet, j_\circ)\}$ incident to $i_\bullet$ cross all edges of $\mathrm{G}^\varepsilon_{I_\bullet, J_\circ} \smallsetminus \{(i_\bullet, j_\circ)\}$ incident to $j_\circ$. Consider now a maximal non-crossing subgraph $\mathtt{t}$ of $\mathrm{G}^\varepsilon_{I_\bullet, J_\circ}$. Then $\mathtt{t}$ contains the edge $(i_\bullet, j_\circ)$ (since $\mathtt{t}$ is maximal) and either $i_\bullet$ or $j_\circ$ is a leaf in $\mathtt{t}$ (since $\mathtt{t}$ is non-crossing). Assume for example that $i_\bullet$ is a leaf and let $I'_\bullet := I_\bullet \smallsetminus \{i_\bullet\}$. Then $\mathtt{t} \smallsetminus \{(i_\bullet, j_\circ)\}$ is a maximal non-crossing subgraph of $\mathrm{G}^\varepsilon_{I'_\bullet, J_\circ}$ (the maximality is ensured from the fact that $(i_\bullet, j_\circ)$ is a boundary edge of $\mathrm{conv}(I_\bullet \cup J_\circ)$). By induction, $\mathtt{t} \smallsetminus \{(i_\bullet, j_\circ)\}$ is thus a spanning tree of $\mathrm{G}^\varepsilon_{I'_\bullet, J_\circ}$, so that $\mathtt{t}$ is a spanning tree of $\mathrm{G}^\varepsilon_{I_\bullet, J_\circ}$. □

In accordance to Proposition 1, we define a *$(\varepsilon, I_\bullet, J_\circ)$-forest* to be a non-crossing subgraph of $\mathrm{G}^\varepsilon_{I_\bullet, J_\circ}$, and a *$(\varepsilon, I_\bullet, J_\circ)$-tree* to be a maximal $(\varepsilon, I_\bullet, J_\circ)$-forest. Note that a $(\varepsilon, I_\bullet, J_\circ)$-tree has $|I_\bullet| + |J_\circ| - 1$ edges. Examples can be found in Figure 2.

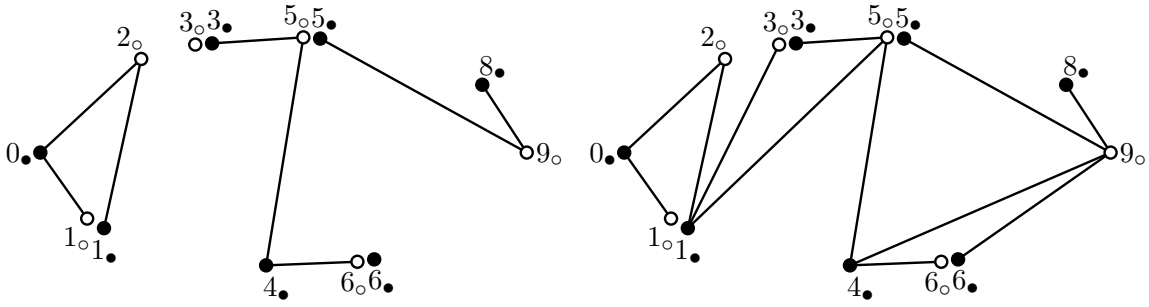


FIGURE 2. A $(\varepsilon, I_\bullet, J_\circ)$-forest (left) and a $(\varepsilon, I_\bullet, J_\circ)$-tree (right) for $\varepsilon = -++-+--+$, $I_\bullet = [\![8_\bullet]\!] \smallsetminus \{2_\bullet, 7_\bullet\}$ and $J_\circ = [\![8_\circ]\!] \smallsetminus \{4_\circ, 7_\circ, 8_\circ\}$.

2.3. **The $(\varepsilon, I_\bullet, J_\circ)$-complex.** We call *$(\varepsilon, I_\bullet, J_\circ)$-complex* $\mathrm{C}^\varepsilon_{I_\bullet, J_\circ}$ the clique complex of the graph of non-crossing edges of $\mathrm{G}^\varepsilon_{I_\bullet, J_\circ}$. In other words, its ground set is the edge set of $\mathrm{G}^\varepsilon_{I_\bullet, J_\circ}$, its faces are the $(\varepsilon, I_\bullet, J_\circ)$-forests, and its facets are the $(\varepsilon, I_\bullet, J_\circ)$-trees.

We say that an edge $(i_\bullet, j_\circ)$ of $\mathrm{G}^\varepsilon_{I_\bullet, J_\circ}$ is *irrelevant* if it is not crossed by any other edge of $\mathrm{G}^\varepsilon_{I_\bullet, J_\circ}$ (*i.e.* , there is no $i'_\bullet \in I_\bullet$ and $j'_\circ \in J_\circ$ separated by $(i_\bullet, j_\circ)$ and such that $i'_\bullet < j'_\circ$). In particular, all edges of $\mathrm{G}^\varepsilon_{I_\bullet, J_\circ}$ on the boundary of $\operatorname{conv}(I_\bullet \cup J_\circ)$ are irrelevant. Note that all $(\varepsilon, I_\bullet, J_\circ)$-trees contain all irrelevant edges of $\mathrm{G}^\varepsilon_{I_\bullet, J_\circ}$, so that the $(\varepsilon, I_\bullet, J_\circ)$-complex $\mathrm{C}^\varepsilon_{I_\bullet, J_\circ}$ is a pyramid over the irrelevant edges of $\mathrm{G}^\varepsilon_{I_\bullet, J_\circ}$.

Although the next statement will directly follow from Proposition 26, we state and prove it here to develop our understanding on the $(\varepsilon, I_\bullet, J_\circ)$-complex. Recall that a simplicial complex is a *pseudomanifold* when it is *pure* (all its maximal faces have the same dimension) and *thin* (any codimension 1 face is contained in at most two facets).

**Proposition 2.** *The $(\varepsilon, I_\bullet, J_\circ)$-complex $\mathrm{C}^\varepsilon_{I_\bullet, J_\circ}$ is a pseudomanifold.*

*Proof.* The $(\varepsilon, I_\bullet, J_\circ)$-complex $\mathrm{C}^\varepsilon_{I_\bullet, J_\circ}$ is pure of dimension $|I_\bullet| + |J_\circ| - 1$ since all its maximal faces are spanning trees of $\mathrm{G}^\varepsilon_{I_\bullet, J_\circ}$. To show that it is thin, assume by contradiction that a codimension 1 face $\mathsf{f}$ is contained in at least three facets $\mathsf{t} := \mathsf{f} \cup \{(i_\bullet, j_\circ)\}$, $\mathsf{t}' := \mathsf{f} \cup \{(i'_\bullet, j'_\circ)\}$, and $\mathsf{t}'' := \mathsf{f} \cup \{(i''_\bullet, j''_\circ)\}$. By maximality of $\mathsf{t}, \mathsf{t}', \mathsf{t}''$, the edges $(i_\bullet, j_\circ)$, $(i'_\bullet, j'_\circ)$ and $(i''_\bullet, j''_\circ)$ are pairwise crossing and all in the same cell of $\operatorname{conv}(I_\bullet \cup J_\circ) \smallsetminus \mathsf{f}$ (*i.e.* the same connected component of the complement of the edges of $\mathsf{f}$ in $\operatorname{conv}(I_\bullet \cup J_\circ)$). Therefore, $i_\bullet, i'_\bullet, i''_\bullet$ are all smaller than $j_\circ, j'_\circ, j''_\circ$ and we obtain that either $(i_\bullet, j'_\circ)$ or $(i_\bullet, j''_\circ)$ (or both) does not belong to $\mathsf{t}$ and does not cross any edge of $\mathsf{t}$, contradicting the maximality of $\mathsf{t}$. □

We say that two $(\varepsilon, I_\bullet, J_\circ)$-trees $\mathsf{t}$ and $\mathsf{t}'$ are *adjacent*, or related by a *flip*, if they share all but one edge, *i.e.* if there is $(i_\bullet, j_\circ) \in \mathsf{t}$ and $(i'_\bullet, j'_\circ) \in \mathsf{t}'$ such that $\mathsf{t} \smallsetminus \{(i_\bullet, j_\circ)\} = \mathsf{t}' \smallsetminus \{(i'_\bullet, j'_\circ)\}$. See Figure 3. Note that not all edges of a $(\varepsilon, I_\bullet, J_\circ)$-tree $\mathsf{t}$ are flippable: for instance, irrelevant edges of $\mathrm{G}^\varepsilon_{I_\bullet, J_\circ}$ (not crossed by other edges of $\mathrm{G}^\varepsilon_{I_\bullet, J_\circ}$) or edges incident to leaves of $\mathsf{t}$ are never flippable. The following statement characterizes the flippable edges.

**Proposition 3.** *(1) Consider two $(\varepsilon, I_\bullet, J_\circ)$-trees $\mathsf{t}$ and $\mathsf{t}'$ with $\mathsf{t} \smallsetminus \{(i_\bullet, j_\circ)\} = \mathsf{t}' \smallsetminus \{(i'_\bullet, j'_\circ)\}$. Then the edges $(i_\bullet, j'_\circ)$ and $(i'_\bullet, j_\circ)$ are contained in $\mathsf{t}$ and $\mathsf{t}'$.*

*(2) An edge $(i_\bullet, j_\circ)$ of a $(\varepsilon, I_\bullet, J_\circ)$-tree $\mathsf{t}$ is flippable if and only if there exists $i'_\bullet \in I_\bullet$ and $j'_\circ \in J_\circ$ such that $i'_\bullet < j'_\circ$ and both $(i_\bullet, j'_\circ)$ and $(i'_\bullet, j_\circ)$ belong to $\mathsf{t}$.*

*Proof.* Point (1) follows by maximality of $\mathsf{t}$ since any edge of $\mathrm{G}^\varepsilon_{I_\bullet, J_\circ}$ that crosses $(i_\bullet, j'_\circ)$ or $(i'_\bullet, j_\circ)$ also crosses $(i_\bullet, j_\circ)$ or $(i'_\bullet, j'_\circ)$ (or both). This also shows one direction of Point (2). For the other direction, we can observe that $i'_\bullet$ and $j'_\circ$ are separated by $(i_\bullet, j_\circ)$ (since the edges $(i_\bullet, j'_\circ)$ and $(i'_\bullet, j_\circ)$ are non-crossing) and we assume that $j_\circ$ and $j'_\circ$ (resp. $i_\bullet$ and $i'_\bullet$) are two consecutive neighbors of $i_\bullet$ (resp. of $j_\circ$) in $\mathsf{t}$. The edge $(i_\bullet, j_\circ)$ can then be flipped to the edge $(i'_\bullet, j'_\circ)$. □

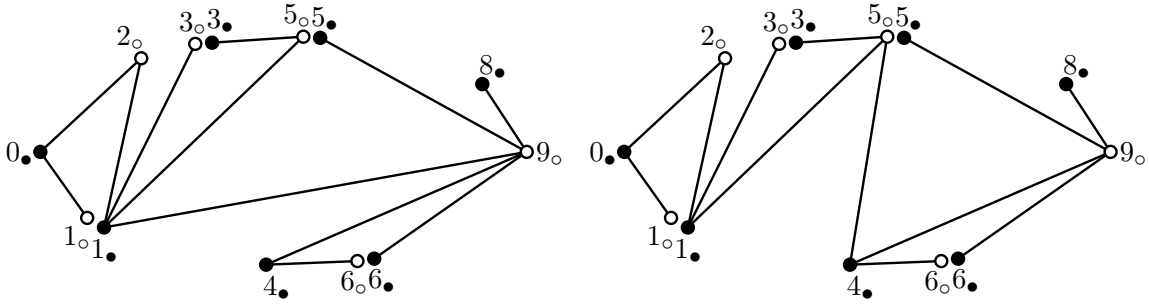


FIGURE 3. Two $(\varepsilon, I_\bullet, J_\circ)$-trees related by a flip. Here, $\varepsilon = -++-+--+$, $I_\bullet = [\![8_\bullet]\!] \smallsetminus \{2_\bullet, 7_\bullet\}$ and $J_\circ = [8_\circ]\!] \smallsetminus \{4_\circ, 7_\circ, 8_\circ\}$.

For instance, the edge $(4_\bullet, 5_\circ)$ of the $(\varepsilon, I_\bullet, J_\circ)$-tree $\mathsf{t}$ of Figure 2 (right) can be flipped to $(1_\bullet, 9_\circ)$ since $(1_\bullet, 5_\circ)$ and $(4_\bullet, 9_\circ)$ belong to $\mathsf{t}$, see Figure 3. In contrast, the edges $(5_\bullet, 9_\circ)$, $(1_\bullet, 3_\circ)$ and $(1_\bullet, 5_\circ)$ of $\mathsf{t}$ are not flippable: the first is irrelevant, the second is incident to a leaf, the last is neither irrelevant nor incident to a leaf but still does not satisfy the condition of Proposition 3 (2).

To conclude, we discuss the boundary of the $(\varepsilon, I_\bullet, J_\circ)$-complex $\mathrm{C}^\varepsilon_{I_\bullet, J_\circ}$. The following lemma characterizes the boundary faces of the $(\varepsilon, I_\bullet, J_\circ)$-complex.

**Lemma 4.** *A $(\varepsilon, I_\bullet, J_\circ)$-forest $\mathsf{f}$ lies on the boundary of the $(\varepsilon, I_\bullet, J_\circ)$-complex $\mathrm{C}^\varepsilon_{I_\bullet, J_\circ}$ if and only if there exists a $(\varepsilon, I_\bullet, J_\circ)$-tree $\mathsf{t}$ with an unflippable edge $\delta$ such that $\mathsf{f} \subseteq \mathsf{t} \smallsetminus \{\delta\}$. In particular, all $(\varepsilon, I_\bullet, J_\circ)$-forests with a missing irrelevant edge or an isolated node lie on the boundary of $\mathrm{C}^\varepsilon_{I_\bullet, J_\circ}$.*

*Proof.* By definition, the codimension 1 faces on the boundary of $\mathrm{C}^\varepsilon_{I_\bullet, J_\circ}$ are precisely the faces of the form $\mathsf{t} \smallsetminus \{\delta)\}$ where $\mathsf{t}$ is a $(\varepsilon, I_\bullet, J_\circ)$-tree and $\delta$ is an unflippable edge of $\mathsf{t}$. The first statement thus immediately follows. Finally, any $(\varepsilon, I_\bullet, J_\circ)$-forest $\mathsf{f}$ with a missing relevant edge $\delta$ (resp. an isolated node $v$) can be completed into a tree $\mathsf{t}$ where $\delta$ is unflippable (resp. where $v$ is a leaf) and $\mathsf{f} \subseteq \mathsf{t} \smallsetminus \{\delta\}$ (resp. $\mathsf{f} \subseteq \mathsf{t} \smallsetminus \{v\}$). □

For instance, consider the $(\varepsilon, I_\bullet, J_\bullet)$-forest $\mathsf{f}$ and the $(\varepsilon, I_\bullet, J_\bullet)$-tree $\mathsf{t}$ of Figure 2. The forest $\mathsf{f}$ lies on the boundary of $\mathrm{C}^\varepsilon_{I_\bullet, J_\circ}$ as it can be completed into $\mathsf{t} \smallsetminus \{(6_\bullet, 9_\circ)\}$ (the irrelevant edge $(6_\circ, 9_\bullet)$ is missing), $\mathsf{t} \smallsetminus \{(1_\bullet, 3_\circ)\}$ (the vertex $3_\circ$ is isolated) or $\mathsf{t} \smallsetminus \{(1_\bullet, 5_\circ)\}$. The $(\varepsilon, I_\bullet, J_\circ)$-forests which are not on the boundary of the $(\varepsilon, I_\bullet, J_\circ)$-complex $\mathrm{C}^\varepsilon_{I_\bullet, J_\circ}$ are called *internal $(\varepsilon, I_\bullet, J_\circ)$-forests*.

2.4. **$\varepsilon$-trees versus triangulations of $\mathrm{P}^\varepsilon_\square$.** We now focus on the situation where $I_\bullet = [\![n_\bullet]\!]$ and $J_\circ = [n_\circ]\!]$. We write $\mathrm{G}^\varepsilon$ for $\mathrm{G}^\varepsilon_{[\![n_\bullet]\!], [n_\circ]\!]}$ and we just call *$\varepsilon$-trees* (resp. forests, resp. complex) the $(\varepsilon, [\![n_\bullet]\!], [n_\circ]\!])$-trees (resp. forests, resp. complex). The following immediate bijection between triangulations of $\mathrm{P}^\varepsilon_\square$ and $\varepsilon$-trees is illustrated in Figure 4.

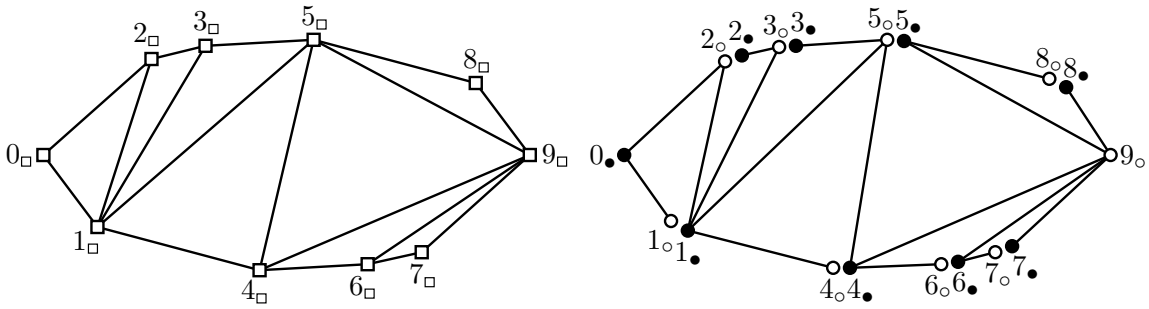


FIGURE 4. A triangulation $T$ of $\mathrm{P}^\varepsilon_\square$ (left) and the corresponding $\varepsilon$-tree $\phi(T)$ (right).

**Proposition 5.** *The map $\phi$ defined by $\phi\big((i_\square, j_\square)\big) = (i_\bullet, j_\circ)$ (for $i_\bullet < j_\circ$) is a bijection between the diagonals of $\mathrm{P}^\varepsilon_\square$ and the edges of $\mathrm{G}^\varepsilon$ and induces a bijection between the dissections (resp. triangulations) of $\mathrm{P}^\varepsilon_\square$ and the $\varepsilon$-forests (resp. $\varepsilon$-trees). In particular, the $\varepsilon$-complex is a simplicial associahedron.*

*Proof.* The map $\phi$ is clearly bijective and sends crossing (resp. non-crossing) diagonals of $\mathrm{P}^\varepsilon_\square$ to crossing (resp. non-crossing) edges of $\mathrm{G}^\varepsilon$. Therefore, it sends dissections of $\mathrm{P}^\varepsilon_\square$ to $\varepsilon$-forests. Finally, it sends triangulations of $\mathrm{P}^\varepsilon_\square$ to $\varepsilon$-trees since a triangulation of $\mathrm{P}^\varepsilon_\square$ has $2n+1$ diagonals (including the boundary edges of $\mathrm{P}^\varepsilon_\square$) and a $\varepsilon$-tree has $2n+1$ edges. □

**Corollary 6.** *For any signature $\varepsilon \in \{\pm\}^n$, there are $\mathrm{cat}(n) := \frac{1}{n+1}\binom{2n}{n}$ many $\varepsilon$-trees.*

2.5. **Non-crossing matchings.** We conclude this section with another family of non-crossing subgraphs of $\mathrm{G}^\varepsilon_{I_\bullet, J_\circ}$ that will be needed later in the proof of Proposition 26. A *perfect matching* of $\mathrm{G}^\varepsilon_{I_\bullet, J_\circ}$ is a subset $M$ of edges of $\mathrm{G}^\varepsilon_{I_\bullet, J_\circ}$ such that each vertex of $\mathrm{G}^\varepsilon_{I_\bullet, J_\circ}$ is contained in precisely one edge of $M$. The following statement is immediate.

**Lemma 7.** *The bipartite graph $\mathrm{G}^\varepsilon_{I_\bullet, J_\circ}$ admits a perfect matching if and only if $|I_\bullet| = |J_\circ|$ and $|I_\bullet \cap [\![k_\bullet]\!]| \geq |J_\circ \cap [k_\circ]\!]|$ for all $k \in [n]$.*

A matching is *non-crossing* if any two of its edges are non-crossing. See Figure 5.

**Lemma 8.** *If $\mathrm{G}^\varepsilon_{I_\bullet, J_\circ}$ admits a perfect matching, then it has a unique non-crossing perfect matching.*

*Proof.* We give an algorithm to construct the unique non-crossing perfect matching of $\mathrm{G}^\varepsilon_{I_\bullet, J_\circ}$. We consider a vertical pile $P$ initially empty. We then read the vertices of $I_\bullet \cup J_\circ$ from left to right (*i.e.* in increasing order and with $i_\circ$ preceding $i_\bullet$ if they both belong to $I_\bullet \cup J_\circ$). At each step, we read a new vertex $k$ and proceed as follows:

- If $k \in I_\bullet$, we insert $k$ on top of $P$ if $\varepsilon_k = +$ and at the bottom of $P$ if $\varepsilon_k = -$.
- If $k \in J_\circ$, then we remove the element $\ell$ on top of $P$ if $\varepsilon_k = +$ and at the bottom of $P$ if $\varepsilon_k = -$, and connect $k$ to $\ell$.

This algorithm clearly terminates and returns a non-crossing matching, assuming that the pile $P$ is never empty when an element of $J_\circ$ is found. This assumption is ensured by the condition $|I_\bullet \cap [\![k_\bullet]\!]| \geq |J_\circ \cap [k_\circ]\!]|$ for all $k \in [n]$. To see that it constructs the unique non-crossing matching, observe that when a vertex $k \in J_\circ$ is found, we have no other choice than connecting it immediately to the last available vertex on top of $P$ if $\varepsilon_k = +$ and at the bottom of $P$ if $\varepsilon_k = -$. Indeed, any other choice would separate some vertices of $P$ to the remaining vertices of $J_\circ$, and thus ultimately lead to a matching with crossings. □

**Remark 9.** Note that Lemma 8 provides another proof that non-crossing subgraphs of $\mathrm{G}^\varepsilon_{I_\bullet, J_\circ}$ are acyclic. Indeed, since $\mathrm{G}^\varepsilon_{I_\bullet, J_\circ}$ is bipartite, any non-crossing cycle could be decomposed into two distinct non-crossing matchings, contradicting Lemma 8.

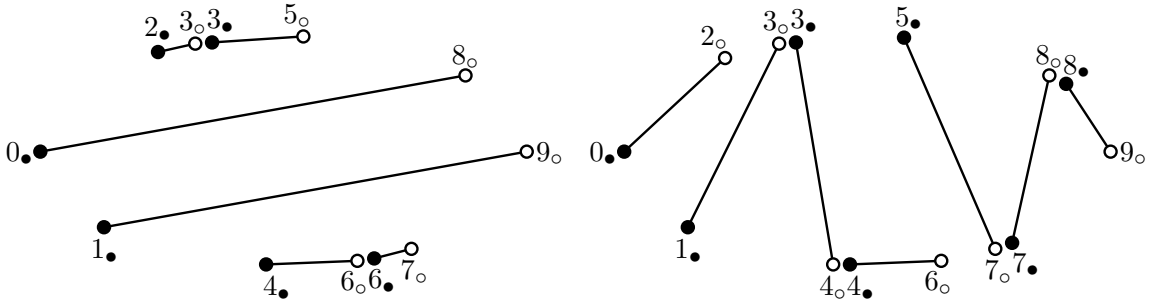


FIGURE 5. The unique non-crossing matching of $\mathrm{G}^\varepsilon_{I_\bullet, J_\circ}$ for two distinct instances of $I_\bullet$ and $J_\circ$.

## 3. The $(\varepsilon, I_\bullet, J_\circ)$-lattice

In this section, we orient flips between $(\varepsilon, I_\bullet, J_\circ)$-trees as follows.

**Lemma 10.** *Consider two adjacent $(\varepsilon, I_\bullet, J_\circ)$-trees $\mathsf{t}$ and $\mathsf{t}'$ with $\mathsf{t} \smallsetminus \{(i_\bullet, j_\circ)\} = \mathsf{t}' \smallsetminus \{(i'_\bullet, j'_\circ)\}$. We say that the flip from $\mathsf{t}$ to $\mathsf{t}'$ is slope increasing (or simply increasing) when the following equivalent conditions hold:*

*(1) the slope of $(i_\bullet, j_\circ)$ is smaller than the slope of $(i'_\bullet, j'_\circ)$,*
*(2) $i'_\bullet$ lies below (resp. $j'_\circ$ lies above) the line passing through $i_\bullet$ and $j_\circ$,*
*(3) the path $j'_\circ i_\bullet j_\circ i'_\bullet$ in $\mathsf{t}$ forms an $\Sigma$ (resp. the path $i_\bullet j'_\circ i'_\bullet j_\circ$ in $\mathsf{t}'$ forms a $\mathsf{Z}$).*

*Otherwise, the flip is called slope decreasing (or simply decreasing).*

We leave the immediate proof of this observation to the reader. For example, the flip of Figure 3 is slope increasing from left to right. In this section, we show that the $(\varepsilon, I_\bullet, J_\circ)$-increasing flip graph is always an interval of the $\varepsilon$-Cambrian lattice of N. Reading [Rea06].

### 3.1. The $(\varepsilon, I_\bullet, J_\circ)$-increasing flip graph.

We call $(\varepsilon, I_\bullet, J_\circ)$-*increasing flip graph* and denote by $\mathrm{F}^\varepsilon_{I_\bullet, J_\circ}$ the oriented graph whose vertices are the $(\varepsilon, I_\bullet, J_\circ)$-trees and whose arcs are increasing flips between them. An example is represented in Figure 7. This section is devoted to some natural properties of this graph, which will be used in the next section to show that the increasing flip graph is the Hasse diagram of a lattice.

Note already that $\mathrm{F}^\varepsilon_{I_\bullet, J_\circ}$ really depends on $(I_\bullet, J_\circ)$, not only on the relative order of the black and white vertices around $\mathrm{conv}(I_\bullet \cup J_\circ)$. As an illustration, when $I_\bullet = [\![n_\bullet]$ and $J_\circ = [n_\circ]\!]$, the black and white vertices are just alternating along $\mathrm{P}^\varepsilon_{\bullet\circ}$, but we will see in Lemma 16 that $\mathrm{F}^\varepsilon_{[\![n_\bullet],[n_\circ]\!]}$ is the Hasse diagram of the $\varepsilon$-Cambrian lattice which really depends on $\varepsilon$.

We start with some symmetries on $(\varepsilon, I_\bullet, J_\circ)$-increasing flip graphs which will save us later work. For a signature $\varepsilon \in \{\pm\}^n$, denote by $\varepsilon^\updownarrow$ and $\varepsilon^\leftrightarrow$ the signatures of $\{\pm\}^n$ defined by $\varepsilon^\updownarrow_k := -\varepsilon_k$ and $\varepsilon^\leftrightarrow_k := \varepsilon_{n+1-k}$ for all $k \in [n]$. For $I_\bullet \subseteq [\![n_\bullet]$ and $J_\circ \subseteq [n_\circ]\!]$, define $I^\leftrightarrow_\bullet := \{(n+1-i)_\circ \mid i_\bullet \in I_\bullet\}$ and $J^\leftrightarrow_\circ := \{(n+1-j)_\bullet \mid j_\circ \in J_\circ\}$.

**Lemma 11.** *The $(\varepsilon^\updownarrow, I_\bullet, J_\circ)$- and $(\varepsilon^\leftrightarrow, J^\leftrightarrow_\circ, I^\leftrightarrow_\bullet)$-increasing flip graphs are both isomorphic to the opposite of the $(\varepsilon, I_\bullet, J_\circ)$-increasing flip graph.*

*Proof.* The horizontal and vertical reflections both exchange the flip directions. □

Let $\mathsf{tmin}^\varepsilon_{I_\bullet, J_\circ}$ (resp. $\mathsf{tmax}^\varepsilon_{I_\bullet, J_\circ}$) denote the set of edges $\delta$ of $\mathrm{G}^\varepsilon_{I_\bullet, J_\circ}$ such that there is no edge of $\mathrm{G}^\varepsilon_{I_\bullet, J_\circ}$ crossing $\delta$ with a smaller (resp. bigger) slope than $\delta$. See Figure 6 for an example.

**Lemma 12.** *The sets $\mathsf{tmin}^\varepsilon_{I_\bullet, J_\circ}$ and $\mathsf{tmax}^\varepsilon_{I_\bullet, J_\circ}$ are $(\varepsilon, I_\bullet, J_\circ)$-trees*

*Proof.* We prove the statement for $\mathsf{tmin}^\varepsilon_{I_\bullet, J_\circ}$, the statement for $\mathsf{tmax}^\varepsilon_{I_\bullet, J_\circ}$ follows by symmetry. The set $\mathsf{tmin}^\varepsilon_{I_\bullet, J_\circ}$ is clearly non-crossing since among any two crossing edges of $\mathrm{G}^\varepsilon_{I_\bullet, J_\circ}$, only the

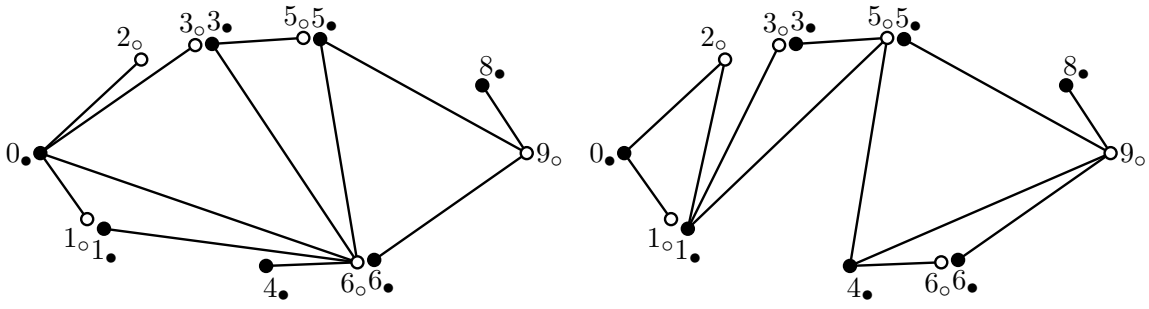


FIGURE 6. The minimal (left) and maximal (right) $(\varepsilon, I_\bullet, J_\circ)$-trees. Here, $\varepsilon = -++-+--+$, $I_\bullet = [\![8_\bullet] \smallsetminus \{2_\bullet, 7_\bullet\}$ and $J_\circ = [8_\circ]\!] \smallsetminus \{4_\circ, 7_\circ, 8_\circ\}$.

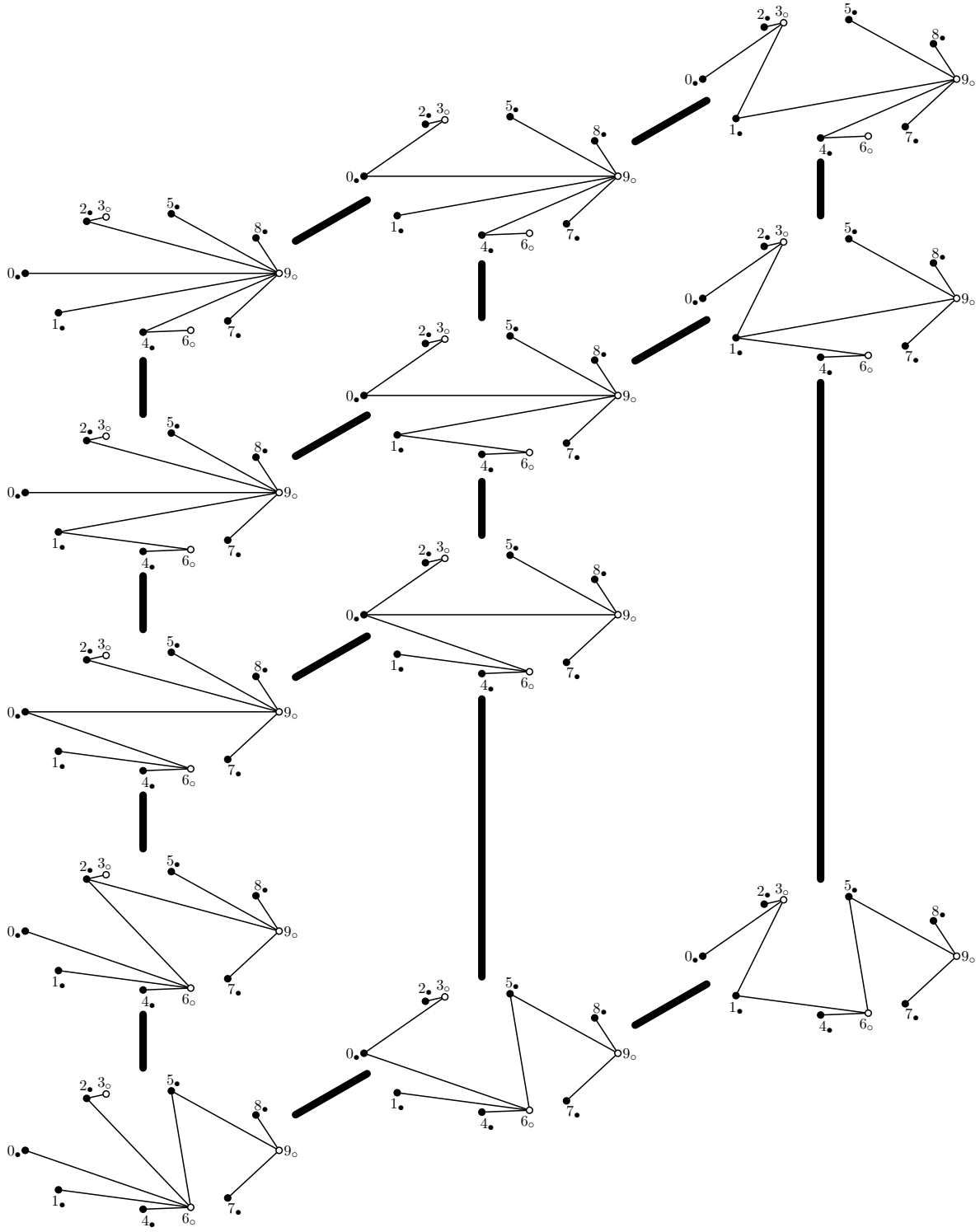

FIGURE 7. The $(\varepsilon, I_\bullet, J_\circ)$-lattice on $(\varepsilon, I_\bullet, J_\circ)$-trees. Increasing flips are oriented upwards. Here, $\varepsilon = -++-+--+$, $I_\bullet = [\![8_\bullet]\!] \smallsetminus \{3_\bullet, 6_\bullet\}$ and $J_\circ = \{3_\circ, 6_\circ, 9_\circ\}$. Compare to Figures 9 and 10.

one of smallest slope can belong to $\mathsf{tmin}^{\varepsilon}_{I_\bullet,J_\circ}$. To see that it is inclusion maximal, consider an edge $(i_\bullet, j_\circ)$ not in $\mathsf{tmin}^{\varepsilon}_{I_\bullet,J_\circ}$. Consider the edge $(i'_\bullet, j'_\circ)$ with the minimal slope among all edges of $\mathrm{G}^{\varepsilon}_{I_\bullet,J_\circ}$ that cross $(i_\bullet, j_\circ)$. If $(i'_\bullet, j'_\circ)$ is not in $\mathsf{tmin}^{\varepsilon}_{I_\bullet,J_\circ}$, it is crossed by an edge $(i''_\bullet, j''_\circ)$ with smaller slope. Then either $(i''_\bullet, j''_\circ)$, or $(i'_\bullet, j''_\circ)$, or $(i''_\bullet, j'_\circ)$ still crosses $(i_\bullet, j_\circ)$ and contradicts the minimality of $(i'_\bullet, j'_\circ)$. We conclude that $(i_\bullet, j_\circ)$ is crossed by an edge of $\mathsf{tmin}^{\varepsilon}_{I_\bullet,J_\circ}$. □

**Proposition 13.** *The $(\varepsilon, I_\bullet, J_\circ)$-increasing flip graph $\mathrm{F}^{\varepsilon}_{I_\bullet,J_\circ}$ is acyclic with a unique source $\mathsf{tmin}^{\varepsilon}_{I_\bullet,J_\circ}$ and a unique sink $\mathsf{tmax}^{\varepsilon}_{I_\bullet,J_\circ}$.*

*Proof.* The $(\varepsilon, I_\bullet, J_\circ)$-increasing flip graph $\mathrm{F}^{\varepsilon}_{I_\bullet,J_\circ}$ is clearly acyclic since an increasing flip increases the sum of the slopes of the edges of the $(\varepsilon, I_\bullet, J_\circ)$-tree.

All flips in $\mathsf{tmin}^{\varepsilon}_{I_\bullet,J_\circ}$ are increasing by definition, so that $\mathsf{tmin}^{\varepsilon}_{I_\bullet,J_\circ}$ is indeed a source. Conversely, any $(\varepsilon, I_\bullet, J_\circ)$-tree $\mathsf{t}$ distinct from $\mathsf{tmin}^{\varepsilon}_{I_\bullet,J_\circ}$ has a decreasing flip. Indeed, we claim that for any edge $(i_\bullet, j_\circ) \in \mathsf{tmin}^{\varepsilon}_{I_\bullet,J_\circ} \smallsetminus \mathsf{t}$, the edge $(i'_\bullet, j'_\circ)$ with maximal slope among the edges of $\mathsf{t}$ that cross $(i_\bullet, j_\circ)$ is flippable and its flip is decreasing. To see it, observe first that there exists $i''_\bullet \in I_\bullet$ strictly above the line $(i'_\bullet, j'_\circ)$ such that $(i''_\bullet, j'_\circ)$ belongs to $\mathsf{t}$ and $i''_\bullet \le \max(i_\bullet, i'_\bullet)$ . Indeed, take either $i_\bullet$ or the black endpoint of the edge of $\mathsf{t}$ crossing $(i_\bullet, j'_\circ)$ closest to $j'_\circ$. Similarly, there exists $j''_\circ \in J_\circ$ strictly below the line $(i'_\bullet, j'_\circ)$ such that $(i'_\bullet, j''_\circ)$ belongs to $\mathsf{t}$ and $j''_\circ \ge \min(j_\circ, j'_\circ)$. Since $i''_\bullet < j''_\circ$ and $(i''_\bullet, j'_\circ)$ and $(i'_\bullet, j''_\circ)$ both belong to $\mathsf{t}$, the edge $(i'_\bullet, j'_\circ)$ is flippable by Proposition 3 (2), and since $i''_\bullet$ is above $(i'_\bullet, j'_\circ)$ while $j''_\circ$ is below $(i'_\bullet, j'_\circ)$, the flip is decreasing by Lemma 10 (2). We conclude that $\mathsf{tmin}^{\varepsilon}_{I_\bullet,J_\circ}$ is the unique source of the $(\varepsilon, I_\bullet, J_\circ)$-increasing flip graph. The proof is symmetric for $\mathsf{tmax}^{\varepsilon}_{I_\bullet,J_\circ}$. □

We conclude with a property of the links of the $(\varepsilon, I_\bullet, J_\circ)$-complex. This property was recently coined *non-revisiting chain property* in [BM18] in the context of graph associahedra.

**Proposition 14.** *The set of $(\varepsilon, I_\bullet, J_\circ)$-trees containing any given $(\varepsilon, I_\bullet, J_\circ)$-forest forms an interval of the $(\varepsilon, I_\bullet, J_\circ)$-increasing flip graph $\mathrm{F}^{\varepsilon}_{I_\bullet,J_\circ}$.*

*Proof.* Consider a $(\varepsilon, I_\bullet, J_\circ)$-forest $\mathsf{f}$. Denote by $C^1, \dots, C^p$ the cells of $\mathsf{f}$ (*i.e.* the closures of the connected components of the complement of $\mathsf{f}$ in $\mathrm{conv}(I_\bullet \cup J_\circ)$). For $k \in [p]$, define $I^k_\bullet := I_\bullet \cap C^k$ and $J^k_\circ := J_\circ \cap C^k$. Then the subgraph of the $(\varepsilon, I_\bullet, J_\circ)$-increasing flip graph $\mathrm{F}^{\varepsilon}_{I_\bullet,J_\circ}$ induced by the $(\varepsilon, I_\bullet, J_\circ)$-trees containing $\mathsf{f}$ is isomorphic to the Cartesian product $\mathrm{F}^{\varepsilon}_{I^1_\bullet,J^1_\circ} \times \cdots \times \mathrm{F}^{\varepsilon}_{I^p_\bullet,J^p_\circ}$. We claim that it actually coincides with the interval of the $(\varepsilon, I_\bullet, J_\circ)$-increasing flip graph $\mathrm{F}^{\varepsilon}_{I_\bullet,J_\circ}$ between $\mathsf{f} \cup \mathsf{tmin}^{\varepsilon}_{I^1_\bullet,J^1_\circ} \cup \cdots \cup \mathsf{tmin}^{\varepsilon}_{I^p_\bullet,J^p_\circ}$ and $\mathsf{f} \cup \mathsf{tmax}^{\varepsilon}_{I^1_\bullet,J^1_\circ} \cup \cdots \cup \mathsf{tmax}^{\varepsilon}_{I^p_\bullet,J^p_\circ}$. For this, we just need to prove that there is no chain of increasing flips that flips out an edge $\delta$ and later flips back in $\delta$.

Consider two adjacent $(\varepsilon, I_\bullet, J_\circ)$-trees $\mathsf{t}$ and $\mathsf{t}'$ with $\mathsf{t} \smallsetminus \{(i_\bullet, j_\circ)\} = \mathsf{t}' \smallsetminus \{(i'_\bullet, j'_\circ)\}$ such that the flip from $\mathsf{t}$ to $\mathsf{t}'$ is increasing. We claim that any edge $\delta$ of $\mathrm{G}^{\varepsilon}_{I_\bullet,J_\circ}$ crossing an edge $\gamma$ of $\mathsf{t}$ with bigger slope also crosses an edge $\gamma'$ of $\mathsf{t}'$ with bigger slope. Indeed, if $\gamma \ne (i_\bullet, j_\circ)$, then $\gamma$ still belongs to $\mathsf{t}'$ and $\gamma' = \gamma$ suits. If $\gamma = (i_\bullet, j_\circ)$, then $\delta \ne (i'_\bullet, j'_\circ)$ since the slope of $\delta$ is smaller than that of $\gamma = (i_\bullet, j_\circ)$ which is in turn smaller than that of $(i'_\bullet, j'_\circ)$. Therefore, $\delta$ must cross two boundary edges of the square $i_\bullet i'_\bullet j_\circ j'_\circ$. Since $\delta$ crosses $(i_\bullet, j_\circ)$, it thus crosses either $(i'_\bullet, j'_\circ)$, or $(i_\bullet, j'_\circ)$, or $(i'_\bullet, j_\circ)$, or the three of them (in which case we choose $\gamma' = (i'_\bullet, j'_\circ)$). Note that these three edges belong to $\mathsf{t}'$ by Proposition 3 (1). Moreover, the slope of $\delta$ is still smaller than the slope of $\gamma'$.

Consider now a sequence $\mathsf{t}_1, \dots, \mathsf{t}_p$ of $(\varepsilon, I_\bullet, J_\circ)$-trees related by increasing flips. Assume that an edge $\delta$ is flipped out from $\mathsf{t}_k$ to $\mathsf{t}_{k+1}$. Then $\delta$ crosses an edge of $\mathsf{t}_{k+1}$ with bigger slope, and thus by induction it crosses an edge of $\mathsf{t}_\ell$ with bigger slope for any $\ell > k$. Therefore, $\delta$ cannot be flipped back in by an increasing flip. □

3.2. **The $(\varepsilon, I_\bullet, J_\circ)$-lattice.** The goal of this section is to prove the following statement.

**Theorem 15.** *The $(\varepsilon, I_\bullet, J_\circ)$-increasing flip graph $\mathrm{F}^{\varepsilon}_{I_\bullet,J_\circ}$ is the Hasse diagram of a lattice, called $(\varepsilon, I_\bullet, J_\circ)$-lattice and denoted by $\mathrm{L}^{\varepsilon}_{I_\bullet,J_\circ}$.*

We start by considering the case when $I_\bullet = [\![n_\bullet]\!]$ and $J_\circ = [n_\circ]\!]$. Recall that two triangulations $T$ and $T'$ of $\mathrm{P}^{\varepsilon}_{\square}$ are related by an increasing flip if there exist diagonals $\delta \in T$ and $\delta' \in T'$ such

that $T \smallsetminus \{\delta\} = T' \smallsetminus \{\delta'\}$ and the slope of $\delta$ is smaller than the slope of $\delta'$. It is known that the transitive closure of the increasing flip graph is a lattice, called the *$\varepsilon$-Cambrian lattice* [Rea06].

**Lemma 16.** *The bijection $\phi$ or Proposition 5 between triangulations of $\mathrm{P}^\varepsilon_\square$ and $\varepsilon$-trees preserves increasing flips. Therefore, the transitive closure of the increasing flip graph on $\varepsilon$-trees is isomorphic to the $\varepsilon$-Cambrian lattice.*

In the classical Tamari case when $\varepsilon = -^n$, the $(I_\bullet, J_\circ)$-lattice is isomorphic to the $\nu(I_\bullet, J_\circ)$-Tamari lattice of [PRV17] for some Dyck path $\nu(I_\bullet, J_\circ)$ described in details in [CPS18, Sect. 3]. Moreover, it is always an interval of the Tamari lattice. We will prove Theorem 15 via the following generalization of this statement.

**Theorem 17.** *The $(\varepsilon, I_\bullet, J_\circ)$-lattice $\mathrm{L}^\varepsilon_{I_\bullet, J_\circ}$ is an interval of the $\varepsilon$-Cambrian lattice.*

In fact, computational experiments indicate the following generalization of Theorem 17.

**Conjecture 18.** *For any $I_\bullet \subseteq I'_\bullet$ and $J_\circ \subseteq J'_\circ$, the $(\varepsilon, I_\bullet, J_\circ)$-lattice $\mathrm{L}^\varepsilon_{I_\bullet, J_\circ}$ is an interval of the $(\varepsilon, I'_\bullet, J'_\circ)$-lattice $\mathrm{L}^\varepsilon_{I'_\bullet, J'_\circ}$.*

Although we are not able to prove Conjecture 18 in full generality, we will prove Theorem 17 using the following three special cases of Conjecture 18.

**Lemma 19.** *For any $K \subseteq [n]$, the $(\varepsilon, [\![n_\bullet]\!] \smallsetminus K_\bullet, [n_\circ]\!] \smallsetminus K_\circ)$-lattice is an interval of the $\varepsilon$-Cambrian lattice.*

*Proof.* For any vertex $k \in K$, let $\delta(k)$ be the edge of $\mathrm{G}^\varepsilon$ joining the vertex of $[\![n_\bullet]\!]$ preceding $k$ to the vertex of $[n_\circ]\!] \smallsetminus K_\circ$ following $k$ on the boundary of $\mathrm{P}^\varepsilon_{\bullet\circ}$. For instance, if $K = \{1, 3, 5, 7\}$ in Figure 1, we obtain $\delta(1) = 0_\bullet 4_\circ$, $\delta(3) = 2_\bullet 8_\circ$, $\delta(5) = 3_\bullet 8_\circ$ and $\delta(7) = 6_\bullet 9_\circ$. The $(\varepsilon, [\![n_\bullet]\!] \smallsetminus K_\bullet, [n_\circ]\!] \smallsetminus K_\circ)$-increasing flip graph is clearly isomorphic to the subgraph of the $(\varepsilon, [\![n_\bullet]\!], [n_\circ]\!])$-increasing flip graph induced by the $(\varepsilon, [\![n_\bullet]\!], [n_\circ]\!])$-trees containing $\{\delta(k) \mid k \in K\}$. Indeed, the edge $\delta(k)$ chops off vertex $k$ as it ensures that the only edges incident to $k_\circ$ and $k_\bullet$ are boundary edges and edges of the form $\delta(k')$ for other $k' \in K$. Therefore, the $(\varepsilon, [\![n_\bullet]\!] \smallsetminus K_\bullet, [n_\circ]\!] \smallsetminus K_\circ)$-lattice is an interval of the $\varepsilon$-Cambrian lattice by Proposition 14 and Lemma 16. □

**Lemma 20.** *For any boundary edge $(i_\bullet, j_\circ)$ of $\mathrm{conv}(I_\bullet \cup J_\circ)$ with $i_\bullet \neq \min(I_\bullet)$ (resp. $j_\circ \neq \max(J_\circ)$), the $(\varepsilon, I_\bullet \smallsetminus \{i_\bullet\}, J_\circ)$-lattice (resp. $(\varepsilon, I_\bullet, J_\circ \smallsetminus \{j_\circ\})$-lattice) is an interval of the $(\varepsilon, I_\bullet, J_\circ)$-lattice.*

*Proof.* By Lemma 11, it is enough to prove that $(\varepsilon, I_\bullet, J_\circ \smallsetminus \{j_\circ\})$-lattice is an interval of the $(\varepsilon, I_\bullet, J_\circ)$-lattice when $j_\circ$ is distinct from $\max(J_\circ)$ and lies on the lower hull of $\mathrm{conv}(I_\bullet \cup J_\circ)$. The $(\varepsilon, I_\bullet, J_\circ \smallsetminus \{j_\circ\})$-increasing flip graph is clearly isomorphic to the subgraph of the $(\varepsilon, I_\bullet, J_\circ)$-increasing flip graph induced by $(\varepsilon, I_\bullet, J_\circ)$-trees with a leaf at $j_\circ$, or equivalently with an edge $(i_\bullet, k_\circ)$ with $k_\circ > j_\circ$. Let $\ell_\circ$ be the vertex of $J_\circ$ following $j_\circ$ along the boundary of $\mathrm{conv}(I_\bullet \cup J_\circ)$ (which exists since $j_\circ \neq \max(J_\circ)$). Let $\mathsf{tmin}$ denote the minimal $(\varepsilon, I_\bullet, J_\circ)$-tree containing $(i_\bullet, \ell_\circ)$ (which exists by Proposition 14). We claim that the set of $(\varepsilon, I_\bullet, J_\circ)$-trees containing an edge $(i_\bullet, k_\circ)$ with $k_\circ > j_\circ$ is precisely the interval above $\mathsf{tmin}$ in the $(\varepsilon, I_\bullet, J_\circ)$-increasing flip graph. We proceed in two steps, showing both inclusions:

- Observe first that any $(\varepsilon, I_\bullet, J_\circ)$-tree above $\mathsf{tmin}$ contains an edge $(i_\bullet, k_\circ)$ with $k_\circ > j_\circ$. Indeed, this property holds for $\mathsf{tmin}$ (as it contains the edge $(i_\bullet, \ell_\circ)$), and it is preserved by an increasing flip (using Proposition 3 (1)).
- Conversely, consider a $(\varepsilon, I_\bullet, J_\circ)$-tree $\mathsf{t}$ containing an edge $(i_\bullet, k_\circ)$ with $k_\circ > j_\circ$. Let $X$ be the half space bounded by $(i_\bullet, k_\circ)$ containing $\ell_\circ$, and consider $\bar{I}_\bullet := I_\bullet \cap X$, $\bar{J}_\circ = J_\circ \cap X$, and $\bar{\mathsf{t}} = \mathsf{t} \cap X$. Note that the minimal $(\varepsilon, \bar{I}_\bullet, \bar{J}_\circ)$-tree $\mathsf{tmin}^\varepsilon_{\bar{I}_\bullet, \bar{J}_\circ}$ contains $(i_\bullet, \ell_\circ)$. Therefore, using a sequence of decreasing flips from $\bar{\mathsf{t}}$ to $\mathsf{tmin}^\varepsilon_{\bar{I}_\bullet, \bar{J}_\circ}$, we can transform $\mathsf{t}$ into a $(\varepsilon, I_\bullet, J_\circ)$-tree $\mathsf{t}'$ containing $(i_\bullet, \ell_\circ)$. Finally, there is a sequence of decreasing flips from $\mathsf{t}'$ to $\mathsf{tmin}$ since $\mathsf{tmin}$ is the minimal $(\varepsilon, I_\bullet, J_\circ)$-tree containing $(i_\bullet, \ell_\circ)$. □

**Lemma 21.** *For any $i < j < k$ such that $(i_\bullet, j_\circ)$ and $(j_\bullet, k_\circ)$ are boundary edges of $\mathrm{conv}(I_\bullet \cup J_\circ)$, the $(\varepsilon, I_\bullet \smallsetminus \{i_\bullet\}, J_\circ \smallsetminus \{j_\circ\})$- and $(\varepsilon, I_\bullet \smallsetminus \{j_\bullet\}, J_\circ \smallsetminus \{k_\circ\})$-lattices are intervals of the $(\varepsilon, I_\bullet, J_\circ)$-lattice.*

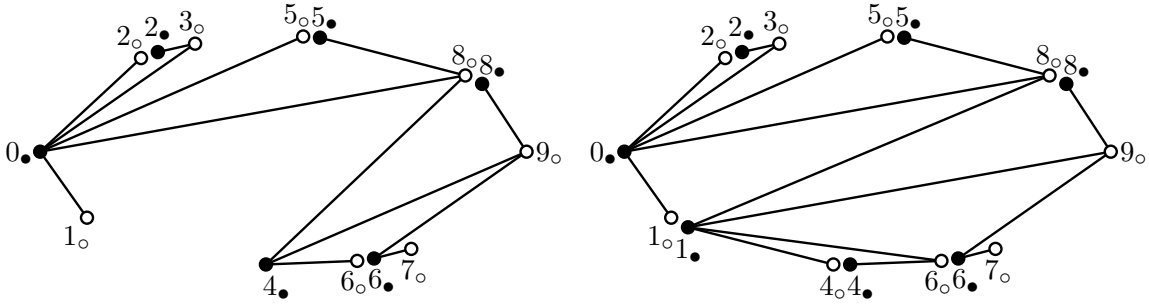


FIGURE 8. The bijection of the proof of Lemma 21. Here, $\varepsilon = -{+}{+}-{+}-{-}{+}$, $I_\bullet = [\![8_\bullet]\!] \smallsetminus \{1_\bullet, 7_\bullet\}$, $J_\circ = [8_\circ] \smallsetminus \{4_\circ\}$, $i = 1$, $j = 4$, and $k = 6$.

*Proof.* By Lemma 11, we can focus on the $(\varepsilon, I_\bullet \smallsetminus \{i_\bullet\}, J_\circ \smallsetminus \{j_\circ\})$-lattice and on the case where $(i_\bullet, j_\circ)$ and $(j_\bullet, k_\circ)$ are lower edges of $\operatorname{conv}(I_\bullet \cup J_\circ)$. The result is also immediate if $i_\bullet = \min(I_\bullet)$, so we assume otherwise. Let $E$ be the set of edges of $\mathrm{G}^\varepsilon_{I_\bullet, J_\circ}$ of the form $(p_\bullet, q_\circ)$ with $p_\bullet < i_\bullet$ and $q_\circ > j_\circ$. Let $(p_\bullet, q_\circ)$ be the edge of maximal slope in $E$.

Let $\mathcal{I}$ be the interval (by Proposition 14) of the $(\varepsilon, I_\bullet, J_\circ)$-increasing flip graph induced by the $(\varepsilon, I_\bullet, J_\circ)$-trees containing $(i_\bullet, k_\circ)$. Let $\mathsf{tmax}$ be the maximal $(\varepsilon, I_\bullet, J_\circ)$-tree of $\mathcal{I}$ containing the edge $(p_\bullet, q_\circ)$ (which exists by Proposition 14). We claim that the interval below $\mathsf{tmax}$ in $\mathcal{I}$ is precisely the set of $(\varepsilon, I_\bullet, J_\circ)$-trees containing $(i_\bullet, k_\circ)$ and an edge of $E$. The proof of this claim, similar to that of Lemma 20 (showing both inclusions), is left to the reader.

Finally, we observe that there is a bijection $\psi$ between the $(\varepsilon, I_\bullet \smallsetminus \{i_\bullet\}, J_\circ \smallsetminus \{j_\circ\})$-trees and the $(\varepsilon, I_\bullet, J_\circ)$-trees containing $(i_\bullet, k_\circ)$ and an edge of $E$. Namely, a $(\varepsilon, I_\bullet \smallsetminus \{i_\bullet\}, J_\circ \smallsetminus \{j_\circ\})$-tree $\mathsf{t}$ is sent to the $(\varepsilon, I_\bullet, J_\circ)$-tree $\phi(\mathsf{t})$ obtained from $\mathsf{t}$ by replacing each edge of the form $(j_\bullet, \ell_\circ)$ by the edge $(i_\bullet, \ell_\circ)$, and finally adding the edges $(i_\bullet, j_\circ)$ and $(j_\bullet, k_\circ)$. See Figure 8. This bijection clearly preserves increasing flips, which concludes the proof. □

*Proof of Theorem 17.* Consider two subsets $I_\bullet \subseteq [\![n_\bullet]\!]$ and $J_\circ \subseteq [n_\bullet]$ such that $\min(I_\bullet) < \min(J_\circ)$ and $\max(I_\bullet) < \max(J_\circ)$. We proceed in three steps:

(1) Let $I'_\bullet$ be the set of points $i_\bullet \notin I_\bullet$ such that $i_\circ$ and the next vertex along the boundary of $\operatorname{conv}(I_\bullet \cup J_\circ)$ belong to $J_\circ$. Similarly, let $J'_\circ$ be the set of points $j_\circ \notin J_\circ$ such that $j_\bullet$ and the previous vertex along the boundary of $\operatorname{conv}(I_\bullet \cup J_\circ)$ belong to $I_\bullet$. By multiple applications of Lemma 20, we obtain that the $(\varepsilon, I_\bullet, J_\circ)$-lattice is an interval of the $(\varepsilon, I_\bullet \cup I'_\bullet, J_\circ \cup J'_\circ)$-lattice.

(2) After the first step, we can assume that the black and white vertices are alternating along the boundary of $\operatorname{conv}(I_\bullet \cup J_\circ)$. Assume that $k_\circ := (n+1)_\circ \notin J_\circ$, consider $j_\circ := \max(J_\circ)$ and let $i_\bullet$ be the minimal vertex of $I_\bullet$ along the same boundary of $\mathrm{P}^\varepsilon_{\bullet\circ}$ as $j_\circ$. Then $(i_\bullet, j_\circ)$ and $(j_\bullet, k_\circ)$ are boundary edges of $\operatorname{conv}(I_\bullet \cup J_\circ \cup \{j_\bullet, k_\circ\})$. Thus, Lemma 21 ensures that the $(\varepsilon, I_\bullet, J_\circ)$-lattice is an interval of the $(\varepsilon, I_\bullet \cup \{j_\bullet\}, J_\circ \cup \{(n+1)_\circ\})$-lattice. A similar argument shows that we can ensure that $0_\bullet \in I_\bullet$.

(3) After the second step, we can assume that $0_\bullet \in I_\bullet$, $(n+1)_\circ \in J_\circ$, and the black and white vertices are alternating along the boundary of $\operatorname{conv}(I_\bullet \cup J_\circ)$. Consider now the set $E$ of edges $(i_\bullet, j_\circ)$ with $i_\bullet \notin I_\bullet$ and $j_\circ \notin J_\circ$, but such that $(i_\circ, j_\bullet)$ is a boundary edge of $\operatorname{conv}(I_\bullet \cup J_\circ)$. Note that each such edge $(i_\bullet, j_\circ)$ is followed by a boundary edge $(j_\bullet, k_\circ)$ of $\operatorname{conv}(I_\bullet \cup J_\circ)$. Let $I'_\bullet$ and $J'_\circ$ be the sets of left and right endpoints of the edges of $E$. By multiple applications of Lemma 21, we obtain that the $(\varepsilon, I_\bullet, J_\circ)$-lattice is an interval of the $(\varepsilon, I_\bullet \cup I'_\bullet, J_\circ \cup J'_\circ)$-lattice.

(4) After the third step, we can assume that $0_\bullet \in I_\bullet$, $(n+1)_\circ \in J_\circ$ and $k_\bullet \in I_\bullet$ if and only if $k_\circ \in J_\circ$ for all $k \in [n]$. Therefore, there is $K \subseteq [n]$ such that $I_\bullet = [\![n_\bullet]\!] \smallsetminus K_\bullet$ and $J_\circ = [n_\circ] \smallsetminus K_\circ$, and we conclude by Lemma 19 that the $(\varepsilon, I_\bullet, J_\circ)$-lattice is an interval of the $\varepsilon$-Cambrian lattice. □

**Remark 22.** It is tempting to attack Conjecture 18 by induction on $|I'_\bullet \smallsetminus I_\bullet| + |J'_\circ \smallsetminus J_\circ|$. By Lemma 11, it would be sufficient to prove that for any $i_\bullet \notin I_\bullet$, the $(\varepsilon, I_\bullet, J_\circ)$-lattice is an interval of the $(\varepsilon, I_\bullet \cup \{i_\bullet\}, J_\circ)$-lattice. Lemma 20 shows this fact in the case when the vertex following $i_\bullet$ along the boundary of $\operatorname{conv}(I_\bullet \cup J_\circ \cup \{i_\bullet\})$ is in $J_\circ$. Lemma 21 treats the case when the two vertices following $i_\bullet$ along the boundary of $\operatorname{conv}(I_\bullet \cup J_\circ \cup \{i_\bullet\})$ are in $I_\bullet$ and $J_\circ$ respectively. However, we did not manage to prove this fact when $i_\bullet$ is followed by two or more vertices of $I_\bullet$ along the boundary of $\operatorname{conv}(I_\bullet \cup J_\circ \cup \{i_\bullet\})$. Note however that we can prove in any case that the $(\varepsilon, I_\bullet, J_\circ)$-lattice is a lattice quotient of an interval of the $(\varepsilon, I_\bullet \cup \{i_\bullet\}, J_\circ)$-lattice.

**Remark 23.** In the classical Tamari case when $\varepsilon = -^n$, the $(I_\bullet, J_\circ)$-increasing flip graph only depends on the sequence of black and white vertices. We can therefore prove Conjecture 18 by induction on $|I'_\bullet \smallsetminus I_\bullet| + |J'_\circ \smallsetminus J_\circ|$ using only Lemma 21. Namely, consider $i_\bullet \notin I_\bullet$, and let $j_\circ$ be the minimal element of $J_\circ$ such that $i_\bullet < j_\circ$. Therefore, there is no vertex of $J_\circ$ in between $i_\bullet$ and $(j-1)_\bullet$. We then distinguish two cases:

- If $(j-1)_\bullet \notin I_\bullet$, then the $(I_\bullet, J_\circ)$-lattice is an interval of the $(I_\bullet \cup \{(j-1)_\bullet\}, J_\circ)$-lattice (by Lemma 21), which is isomorphic to the $(I_\bullet \cup \{i_\bullet\}, J_\circ)$-lattice.
- If $(j-1)_\bullet \in I_\bullet$, then the $(I_\bullet, J_\circ)$-lattice is isomorphic to the $(I_\bullet \cup \{i_\bullet\} \smallsetminus \{(j-1)_\bullet\}, J_\circ)$-lattice, which is an interval of the $(I_\bullet \cup \{i_\bullet\}, J_\circ)$-lattice (by Lemma 21).

A similar argument (or an application of Lemma 11) shows that the $(I_\bullet, J_\circ)$-lattice is an interval of the $(I_\bullet, J_\circ \cup \{j_\circ\})$-lattice for any $j_\circ \notin J_\circ$. We conclude that the $\nu(I_\bullet, J_\circ)$-Tamari lattice is an interval of the $\nu(I'_\bullet, J'_\circ)$-Tamari lattice for any $I_\bullet \subseteq I'_\bullet$ and $J_\circ \subseteq J'_\circ$.

**Remark 24.** There is yet another simple way to prove Theorem 17 in the classical Tamari situation when $\varepsilon = -^n$, based on the canopies of the corresponding dual binary trees.

Consider a triangulation $T$ of $\mathrm{P}^\varepsilon_\square$ and its corresponding $\varepsilon$-tree $\mathsf{t} \coloneqq \phi(T)$. As defined in [LP18, CP17], the *dual Cambrian tree* of $T$ (or of $\mathsf{t}$) is the (oriented and labeled) tree with

- one vertex labeled $j$ for each triangle $i_\square j_\square k_\square$ of $T$ with $i < j < k$,
- one arc between (the vertices corresponding to) any two adjacent triangles, oriented from the triangle below to the triangle above their common diagonal.

The *canopy* of $T$ (or of $\mathsf{t}$) is the sequence of signs $\operatorname{can}(T) = \operatorname{can}(\mathsf{t}) \in \{\pm\}^{n-1}$ defined by $\operatorname{can}(T)_i = -$ is $i$ is below $i+1$ in the dual Cambrian tree of $T$, and $\operatorname{can}(T)_i = +$ otherwise. The canopy is a natural geometric parameter as it corresponds to the position of the cone of $T$ in the $\varepsilon$-Cambrian fan of N. Reading and D. Speyer [RS09] with respect to the hyperplanes orthogonal to the simple roots.

For a $\varepsilon$-tree, there is a connection between its canopy and its leaves. Namely, if $i_\bullet$ is a black leaf of $\mathsf{t}$, then $\operatorname{can}(\mathsf{t})_i \, \varepsilon_i = +$ and similarly, if $j_\circ$ is a white leaf of $\mathsf{t}$, then $\operatorname{can}(\mathsf{t})_{j-1} \, \varepsilon_j = -$. When $\varepsilon = -^n$, the reverse implications hold so that the canopy $\operatorname{can}(\mathsf{t})$ can be read directly on the tree $\mathsf{t}$. In particular, the $(I_\bullet, J_\circ)$-trees can be identified as the $-^n$-trees with particular conditions on their canopy. This enables us to derive easily Theorem 17 when $\varepsilon = -^n$. However, the reverse implications do not always hold for general signatures. For example, the $\varepsilon$-tree $\mathsf{t}$ represented in Figure 4 has $\operatorname{can}(\mathsf{t})_5 \, \varepsilon_5 = +$ while $5_\bullet$ is not a leaf of $\mathsf{t}$.

In particular, while the classical Tamari lattice can be decomposed into smaller $\nu$-Tamari lattices as observed in [PRV17], the $\varepsilon$-Cambrian lattice decomposes into intervals corresponding with $\varepsilon$-trees with the same canopy, but these intervals do not correspond to the $(\varepsilon, I_\bullet, J_\circ)$-lattices.

We conclude this section with a geometric consequence of Theorem 17. Remember that the $\varepsilon$-Cambrian lattice can be realized geometrically as

- the dual graph of the $\varepsilon$-Cambrian fan of N. Reading and D. Speyer [RS09],
- the graph of the $\varepsilon$-associahedron of C. Hohlweg and C. Lange [HL07].

As an interval of the $\varepsilon$-Cambrian lattice gives rise to a connected region of the $\varepsilon$-Cambrian fan, we obtain the following geometric realization of the $(\varepsilon, I_\bullet, J_\circ)$-lattice.

**Corollary 25.** *The $(\varepsilon, I_\bullet, J_\circ)$-increasing flip graph is realized geometrically as the dual graph of a set cones of the $\varepsilon$-Cambrian fan of* [RS09] *corresponding to an interval of the $\varepsilon$-Cambrian lattice.*

## 4. The $(\varepsilon, I_\bullet, J_\circ)$-Cambrian triangulation

In this section, we use $\varepsilon$-trees to construct a flag regular triangulation $\mathcal{T}^\varepsilon$ of the subpolytope $\operatorname{conv}\{(\mathbf{e}_{i_\bullet}, \mathbf{e}_{j_\circ}) \mid 0 \le i_\bullet < j_\circ \le n+1\}$ of the product of simplices $\triangle_{[\![n_\bullet]\!]} \times \triangle_{[n_\circ]\!]}$. Restricting $\mathcal{T}^\varepsilon$ to the face $\triangle_{I_\bullet} \times \triangle_{J_\circ}$ then yields a triangulation whose dual graph is the flip graph on $(\varepsilon, I_\bullet, J_\circ)$-trees.

4.1. **The $\varepsilon$-Cambrian triangulation.** Let $(\mathbf{e}_{i_\bullet})_{i_\bullet \in I_\bullet}$ denote the standard basis of $\mathbb{R}^{I_\bullet}$ and $(\mathbf{e}_{j_\circ})_{j_\circ \in J_\circ}$ denote the standard basis of $\mathbb{R}^{J_\circ}$. We consider the Cartesian product of the two standard simplices

$$\triangle_{I_\bullet} \times \triangle_{J_\circ} := \operatorname{conv}\{(\mathbf{e}_{i_\bullet}, \mathbf{e}_{j_\circ}) \mid i_\bullet \in I_\bullet,\ j_\circ \in J_\circ\}$$

and its subpolytope

$$\mathrm{U}_{I_\bullet, J_\circ} := \operatorname{conv}\{(\mathbf{e}_{i_\bullet}, \mathbf{e}_{j_\circ}) \mid i_\bullet \in I_\bullet,\ j_\circ \in J_\circ \text{ and } i_\bullet < j_\circ\}.$$

Note that the polytopes $\triangle_{I_\bullet} \times \triangle_{J_\circ}$ and $\mathrm{U}_{I_\bullet, J_\circ}$ are faces of the polytopes $\triangle_{[\![n_\bullet]\!]} \times \triangle_{[n_\circ]\!]}$ and $\mathrm{U}_{[\![n_\bullet]\!], [n_\circ]\!]}$ respectively.

**Proposition 26.** *Each $(\varepsilon, I_\bullet, J_\circ)$-tree $\mathtt{t}$ defines a simplex $\triangle_\mathtt{t} := \operatorname{conv}\{(\mathbf{e}_{i_\bullet}, \mathbf{e}_{j_\circ}) \mid (i_\bullet, j_\circ) \in \mathtt{t}\}$ and the collection of simplices $\mathcal{T}^\varepsilon_{I_\bullet, J_\circ} := \{\triangle_\mathtt{t} \mid \mathtt{t}\ (\varepsilon, I_\bullet, J_\circ)\text{-tree}\}$ is a flag triangulation of $\mathrm{U}_{I_\bullet, J_\circ}$, that we call the $\varepsilon$-Cambrian triangulation of $\mathrm{U}_{I_\bullet, J_\circ}$.*

*Proof.* Since a triangulation of a polytope induces a triangulation on all its faces, we only need to prove the result for $I_\bullet = [\![n_\bullet]\!]$ and $J_\circ = [n_\circ]\!]$. Let $\mathrm{U} := \mathrm{U}_{[\![n_\bullet]\!], [n_\circ]\!]}$. Observe that:

- Each $\triangle_\mathtt{t}$ is a full-dimensional simplex since $\mathtt{t}$ is a spanning tree of $\mathrm{G}^\varepsilon$.
- For $\mathtt{t} \neq \mathtt{t}'$, the simplices $\triangle_\mathtt{t}$ and $\triangle_{\mathtt{t}'}$ intersect along a face of both. Otherwise, there exists a vector that can be written both as a positive linear combination of rays of $\triangle_\mathtt{t}$ and as a positive linear combination of rays of $\triangle_{\mathtt{t}'}$. This translates into a linear dependence whose support is a cycle $C$ that alternates between $\mathtt{t}$ and $\mathtt{t}'$. In other words, this provides two distinct non-crossing matchings on the support of $C$, contradicting Lemma 8.
- The total volume of these simplices is the volume of U. On the one hand, since each simplex is unimodular, Corollary 6 shows that the total normalized volume of the simplices is $\operatorname{cat}(n)$. On the other hand, the normalized volume of U is known to be $\operatorname{cat}(n)$ as it is triangulated by the (bottom part of the) staircase triangulation [DRS10, Sect. 6.2.3].

This proves that $\{\triangle_\mathtt{t} \mid \mathtt{t}\ \varepsilon\text{-tree}\}$ is a triangulation of U. It is clearly flag by definition of $\varepsilon$-trees. □

**Remark 27.** Since the $\varepsilon$-Cambrian triangulation only depends on the crossings among the edges of $\mathrm{G}^\varepsilon$, the $\varepsilon^\updownarrow$-Cambrian triangulation coincides with the $\varepsilon$-Cambrian triangulation, while the $\varepsilon^\leftrightarrow$-Cambrian triangulation is the image of the $\varepsilon$-Cambrian triangulation by the symmetry that simultaneously exchanges $\mathbf{e}_{k_\bullet}$ with $\mathbf{e}_{k_\circ}$ for all $k \in [n]$.

**Example 28.** Consider the case $n = 3$. Denote the vertices of U by

$$\begin{array}{cccc} \alpha = (\mathbf{e}_{0_\bullet}, \mathbf{e}_{1_\circ}) & \beta = (\mathbf{e}_{0_\bullet}, \mathbf{e}_{2_\circ}) & \gamma = (\mathbf{e}_{0_\bullet}, \mathbf{e}_{3_\circ}) & \delta = (\mathbf{e}_{0_\bullet}, \mathbf{e}_{4_\circ}) \\ & \epsilon = (\mathbf{e}_{1_\bullet}, \mathbf{e}_{2_\circ}) & \eta = (\mathbf{e}_{1_\bullet}, \mathbf{e}_{3_\circ}) & \kappa = (\mathbf{e}_{1_\bullet}, \mathbf{e}_{4_\circ}) \\ & & \lambda = (\mathbf{e}_{2_\bullet}, \mathbf{e}_{3_\circ}) & \mu = (\mathbf{e}_{2_\bullet}, \mathbf{e}_{4_\circ}) \\ & & & \nu = (\mathbf{e}_{3_\bullet}, \mathbf{e}_{4_\circ}) \end{array}$$

Then the 4 $\varepsilon$-Cambrian triangulations and the staircase triangulation of U are given by the simplices

| $\varepsilon$ | $---$ or $+++$ | $--+$ or $++-$ | $-+-$ or $+-+$ | $-++$ or $+--$ | staircase triang. |
|---|---|---|---|---|---|
| simplices | $\alpha\beta\gamma\delta\epsilon\lambda\nu$ | $\alpha\beta\gamma\delta\epsilon\mu\nu$ | $\alpha\beta\gamma\delta\eta\mu\nu$ | $\alpha\beta\gamma\delta\kappa\lambda\nu$ | $\alpha\beta\gamma\delta\kappa\mu\nu$ |
| | $\alpha\beta\delta\epsilon\lambda\mu\nu$ | $\alpha\beta\gamma\epsilon\lambda\mu\nu$ | $\alpha\beta\gamma\eta\lambda\mu\nu$ | $\alpha\beta\gamma\eta\kappa\lambda\nu$ | $\alpha\beta\gamma\eta\kappa\mu\nu$ |
| | $\alpha\gamma\delta\epsilon\eta\lambda\nu$ | $\alpha\gamma\delta\epsilon\kappa\mu\nu$ | $\alpha\beta\delta\eta\kappa\mu\nu$ | $\alpha\beta\delta\kappa\lambda\mu\nu$ | $\alpha\beta\gamma\eta\lambda\mu\nu$ |
| | $\alpha\delta\epsilon\eta\kappa\lambda\nu$ | $\alpha\gamma\epsilon\eta\kappa\mu\nu$ | $\alpha\beta\epsilon\eta\kappa\mu\nu$ | $\alpha\beta\epsilon\eta\kappa\lambda\nu$ | $\alpha\beta\epsilon\eta\kappa\mu\nu$ |
| | $\alpha\delta\epsilon\kappa\lambda\mu\nu$ | $\alpha\gamma\epsilon\eta\lambda\mu\nu$ | $\alpha\beta\epsilon\eta\lambda\mu\nu$ | $\alpha\beta\epsilon\kappa\lambda\mu\nu$ | $\alpha\beta\epsilon\eta\lambda\mu\nu$ |

**Remark 29.** Note that Proposition 26 provides an alternative proof of Proposition 2.

**Remark 30.** As a corollary of Proposition 26 and the unimodularity of $\mathrm{U}_{I_\bullet,J_\circ}$, we obtain that the number of $(\varepsilon, I_\bullet, J_\circ)$-trees is independent of $\varepsilon$. It is clear for $I_\bullet = [\![n_\bullet]\!]$ and $J_\circ = [\![n_\circ]\!]$ using the bijection of Proposition 5 but we have not found a clear combinatorial reason for general $I_\bullet$ and $J_\circ$.

Finally, we gather two geometric consequences of Proposition 26. The first is just a reformulation of Proposition 26.

**Corollary 31.** *The $(\varepsilon, I_\bullet, J_\circ)$-increasing flip graph is geometrically realized as the dual graph of the triangulation $\mathcal{T}^\varepsilon_{I_\bullet,J_\circ}$.*

The second is an application of the Cayley trick [HRS00] to visualize triangulations of products of simplices as mixed subdivisions of generalized permutahedra. Recall that a *generalized permutahedron* [Pos09, PRW08] is a polytope whose normal fan coarsens the normal fan of the permutahedron $\operatorname{conv}\{(\sigma_1,\dots,\sigma_n) \mid \sigma \in \mathfrak{S}_n\}$. For example, the Minkowski sum $\sum_{I\subseteq[n]} y_I \triangle_I$ is a generalized permutahedron for any family of non-negative real numbers $(y_I)_{I\subseteq[n]}$ (where $\triangle_I := \operatorname{conv}\{\mathbf{e}_i \mid i \in I\}$ denotes the face of the standard simplex corresponding to $I$). The following statement is illustrated in Figure 9.

**Corollary 32.** *The collection of generalized permutahedra $\sum_{i_\bullet\in I_\bullet} \triangle_{\{j_\circ\in J_\circ \mid (i_\bullet,j_\circ)\in \mathsf{t}\}}$, where $\mathsf{t}$ ranges over all $(\varepsilon, I_\bullet, J_\circ)$-trees, forms a coherent fine mixed subdivision of the generalized permutahedron $\sum_{i_\bullet\in I_\bullet} \triangle_{\{j_\circ\in J_\circ \mid i_\bullet<j_\circ\}}$.*

4.2. **Regularity.** Recall that a triangulation $T$ of a point set $P$ is *regular* if there exists a lifting function $h : P \to \mathbb{R}$ such that $T$ is the projection of the lower convex hull of the lifted point set $\{(p, h(p)) \mid p \in P\}$.

**Proposition 33.** *For any $\varepsilon \in \{\pm\}^n$, $I_\bullet \subseteq [\![n_\bullet]\!]$ and $J_\circ \subseteq [\![n_\circ]\!]$, the triangulation $\mathcal{T}^\varepsilon_{I_\bullet,J_\circ}$ is regular.*

*Proof.* Consider two adjacent $\varepsilon$-trees $\mathsf{t},\mathsf{t}'$ with $\mathsf{t} \smallsetminus \{(i_\bullet, j_\circ)\} = \mathsf{t}' \smallsetminus \{(i'_\bullet, j'_\circ)\}$. Then the linear dependence between the vertices of $\triangle_\mathsf{t}$ and $\triangle'_\mathsf{t}$ is given by

$$(\mathbf{e}_{i_\bullet}, \mathbf{e}_{j_\circ}) + (\mathbf{e}_{i'_\bullet}, \mathbf{e}_{j'_\circ}) = (\mathbf{e}_{i_\bullet}, \mathbf{e}_{j'_\circ}) + (\mathbf{e}_{i'_\bullet}, \mathbf{e}_{j_\circ}).$$

Therefore, we just need to find a lifting function $h : \{(i_\bullet, j_\circ) \mid i_\bullet \in I_\bullet,\, j_\circ \in J_\circ,\, i_\bullet < j_\circ\} \to \mathbb{R}$ such that for any two crossing edges $(i_\bullet, j_\circ)$ and $(i'_\bullet, j'_\circ)$ of $\mathrm{G}^\varepsilon$, we have

$$h\big((i_\bullet, j_\circ)\big) + h\big((i'_\bullet, j'_\circ)\big) > h\big((i_\bullet, j'_\circ)\big) + h\big((i'_\bullet, j_\circ)\big).$$

For this, consider any strictly concave increasing function $f : \mathbb{R} \to \mathbb{R}$. For a diagonal $\zeta$ of $\mathrm{P}^\varepsilon_\square$, we denote by $\ell(\zeta)$ the minimum between the number of vertices of $\mathrm{P}^\varepsilon_\square$ on each side of the diagonal $\zeta$. Consider two crossing diagonals $\zeta$ and $\eta$ of $\mathrm{P}^\varepsilon_\square$. These diagonals decompose the polygon $\mathrm{P}^\varepsilon_\square$ into four regions that we denote by $A, B, C, D$ such that $\zeta$ separates $A\cup B$ from $C\cup D$ and $|A\cup B| \le |C\cup D|$, while $\eta$ separates $A\cup C$ from $B\cup D$ and $|A\cup C| \le |B\cup D|$. We also denote accordingly by $\alpha, \beta, \gamma, \delta$ the boundary edges of the square with diagonals $\zeta, \eta$. Thus, we have

$$\ell(\zeta) = |A| + |B| + 1 \qquad \text{and} \qquad \ell(\eta) = |A| + |C| + 1$$

$$\text{while} \qquad \ell(\alpha) = |A|, \qquad \ell(\beta) \le |B|, \qquad \ell(\gamma) \le |C|, \qquad \text{and} \qquad \ell(\delta) \le |A| + |B| + |C| + 2.$$

Using the strict concavity of $f$ for the first inequality and the increasing property of $f$ for the second inequality, we obtain that

$$f(\ell(\zeta)) + f(\ell(\eta)) > f(\ell(\alpha)) + f(\ell(\delta)) \qquad \text{and} \qquad f(\ell(\zeta)) + f(\ell(\eta)) > f(\ell(\beta)) + f(\ell(\gamma)).$$

Finally, we transport this convenient function through the bijection $\phi$ of Proposition 5 to obtain a suitable lifting function $h := f \circ \ell \circ \phi^{-1}$. □

**Remark 34.** In the classical Tamari case when $\varepsilon = -^n$, the function $\ell$ in the proof of Proposition 33 can be replaced by $\ell'\big((i_\bullet, j_\circ)\big) = j_\circ - i_\bullet$. Note however that this simple function $\ell'$ fails for arbitrary signatures $\varepsilon \in \{\pm\}^n$.

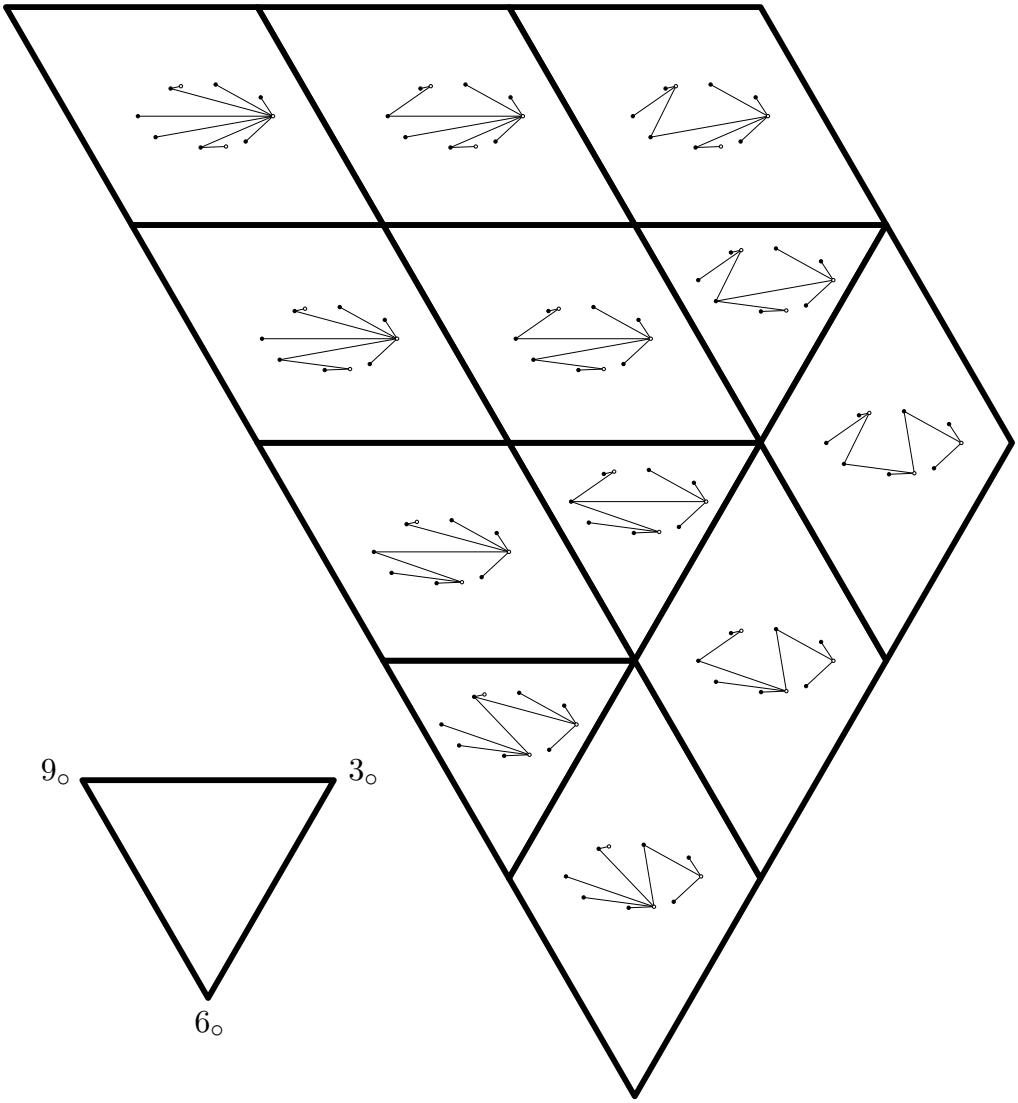


FIGURE 9. The mixed subdivision realization of the $(\varepsilon, I_\bullet, J_\circ)$-lattice. Here, $\varepsilon = -++-+--+$, $I_\bullet = [\![8_\bullet]\!] \smallsetminus \{3_\bullet, 6_\bullet\}$ and $J_\circ = \{3_\circ, 6_\circ, 9_\circ\}$. Compare to Figures 7 and 10.

**Remark 35.** Propositions 26 and 33 enable us to understand $2^{n-1}$ distinct regular triangulations of $\mathrm{U} := \mathrm{U}_{[\![n_\bullet]\!],[\![n_\circ]\!]}$. It would be interesting to investigate if one can understand similarly more (regular) triangulations of U. Note that not all regular triangulations of U are flag. Some computations:

| $n$ | 1 | 2 | 3 | 4 | 5 |
|---|---|---|---|---|---|
| # $\varepsilon$-Cambrian triangulations of U | 1 | 1 | 2 | 4 | 8 |
| # regular triangulations of U | 1 | 1 | 2 | 20 | 3324 |
| # flag regular triangulations of U | 1 | 1 | 2 | 16 | 848 |

## 5. Tropical realization

In this section, we exploit the triangulation $\mathcal{T}^\varepsilon$ to obtain a geometric realization of the $(\varepsilon, I_\bullet, J_\circ)$-lattice as the edge graph of a polyhedral complex induced by a tropical hyperplane arrangement. We follow the same lines as [CPS18], relying on work of M. Develin and B. Sturmfels [DS04]. Define the following geometric objects in the tropical projective space $\mathbb{TP}^{|J_\circ|-1} = \mathbb{R}^{J_\circ}/\mathbb{R}\mathbb{1}$:

(1) For each $i_\bullet \in I_\bullet$, consider the inverted tropical hyperplane at $\big(h(i_\bullet, j_\circ)\big)_{j_\circ \in J_\circ}$ defined by

$$H_{i_\bullet} := \Big\{ x \in \mathbb{TP}^{|J_\circ|-1} \;\Big|\; \max_{j_\circ \in J_\circ} \{x_{j_\circ} - h(i_\bullet, j_\circ)\} \text{ is attained twice} \Big\}.$$

(2) For each edge $(i_\bullet, j_\circ)$ of $\mathrm{G}^\varepsilon_{I_\bullet, J_\circ}$, consider the polyhedron

$$g(i_\bullet, j_\circ) := \big\{ x \in \mathbb{R}^{J_\circ} \;\big|\; x_{k_\circ} - x_{j_\circ} \le h(i_\bullet, k_\circ) - h(i_\bullet, j_\circ) \text{ for each } k_\circ \in J_\circ \big\} \cap \{x_{\max(J_\circ)} = 0\}.$$

(3) For each covering $(\varepsilon, I_\bullet, J_\circ)$-forest $\mathsf{f}$, consider the polyhedron

$$g(\mathsf{f}) := \bigcap_{(i_\bullet, j_\circ) \in \mathsf{f}} g(i_\bullet, j_\circ).$$

(4) For each $(I_\bullet, J_\circ)$-tree $\mathsf{t}$, consider the point $g(\mathsf{t}) \in \mathbb{R}^{J_\circ}$ whose $k_\circ$ coordinate is given by

$$g(\mathsf{t})_{k_\circ} = \sum_{(i_\bullet, j_\circ) \in p(\mathsf{t}, k_\circ)} \pm h(i_\bullet, j_\circ),$$

where $p(\mathsf{t}, k_\circ)$ is the unique path in $\mathsf{t}$ from $k_\circ$ to $\max(J_\circ)$, and the sign of the summand $h(i_\bullet, j_\circ)$ is negative if $p(\mathsf{t}, k_\circ)$ traverses $(i_\bullet, j_\circ)$ from $i_\bullet$ to $j_\circ$ and positive otherwise.

We call $(\varepsilon, I_\bullet, J_\circ)$-*associahedron* the polyhedral complex $\mathsf{Asso}^\varepsilon_{I_\bullet, J_\circ}(h)$ given by the bounded cells of the arrangement of tropical hyperplanes $H_{i_\bullet}$ for $i_\bullet \in I_\bullet$. The following statement is identical to that of [CPS18] and its proof is similar.

**Theorem 36.** *The $(\varepsilon, I_\bullet, J_\circ)$-associahedron $\mathsf{Asso}^\varepsilon_{I_\bullet, J_\circ}(h)$ is a polyhedral complex whose cell poset is anti-isomorphic to the inclusion poset of interior faces of the $(\varepsilon, I_\bullet, J_\circ)$-complex. In particular,*

- *each internal $(\varepsilon, I_\bullet, J_\circ)$-forest $\mathsf{f}$ corresponds to a face $g(\mathsf{f})$ of $\mathsf{Asso}^\varepsilon_{I_\bullet, J_\circ}(h)$;*
- *each $(\varepsilon, I_\bullet, J_\circ)$-tree $\mathsf{t}$ corresponds to a vertex $g(\mathsf{t})$ of $\mathsf{Asso}^\varepsilon_{I_\bullet, J_\circ}(h)$;*
- *each flip corresponds to an edge of $\mathsf{Asso}^\varepsilon_{I_\bullet, J_\circ}(h)$.*

*In particular, the edge graph of $\mathsf{Asso}^\varepsilon_{I_\bullet, J_\circ}(h)$ is the flip graph on $(\varepsilon, I_\bullet, J_\circ)$-trees. In fact, when oriented in the linear direction $-\sum_{j_\circ \in J_\circ \smallsetminus \{\max(J_\circ)\}} x_{j_\circ}$, the edge graph of $\mathsf{Asso}^\varepsilon_{I_\bullet, J_\circ}(h)$ is the increasing flip graph $\mathrm{F}^\varepsilon_{I_\bullet, J_\circ}$ on $(\varepsilon, I_\bullet, J_\circ)$-trees.*

**Remark 37.** It is natural to wonder when is the $(I_\bullet, J_\circ)$-associahedron a polyhedral subdivision of a convex polytope. In the classical Tamari case $\varepsilon = -^n$, the pairs $(I_\bullet, J_\circ)$ for which this property holds are characterized in [CPS18, Thm. 5.12], and it turns out that the support of the $(I_\bullet, J_\circ)$-associahedron is then a classical associahedron. An interesting open problem is thus to determine for which triples $(\varepsilon, I_\bullet, J_\circ)$ is the $(\varepsilon, I_\bullet, J_\circ)$-associahedron a polyhedral subdivision of a convex polytope, and more specifically of an $\varepsilon$-associahedron.

**Example 38.** Consider $\varepsilon = -{+}{+}{-}{+}{-}{-}{+}$, $I_\bullet = [\![8_\bullet]\!] \smallsetminus \{3_\bullet, 6_\bullet\}$ and $J_\circ = \{3_\circ, 6_\circ, 9_\circ\}$. We consider the lifting function $h(i_\bullet, j_\circ) = \sqrt{\ell(i_\square, j_\square)}$ which gives

$$h(i_\bullet, j_\circ) = \begin{array}{c} \begin{array}{ccccccc} 0_\bullet & 1_\bullet & 2_\bullet & 4_\bullet & 5_\bullet & 7_\bullet & 8_\bullet \end{array} \\ \begin{pmatrix} 1 & \sqrt{2} & 0 & \infty & \infty & \infty & \infty \\ \sqrt{2} & 1 & \sqrt{3} & 0 & \sqrt{3} & \infty & \infty \\ 2 & \sqrt{3} & \sqrt{3} & \sqrt{2} & 1 & 0 & 0 \end{pmatrix} \end{array} \begin{array}{c} 3_\circ \\ 6_\circ \\ 9_\circ \end{array}$$

The corresponding tropical hyperplane arrangement is represented in Figure 10. Oriented northeast, it coincides with the increasing flip graph represented in Figure 7.

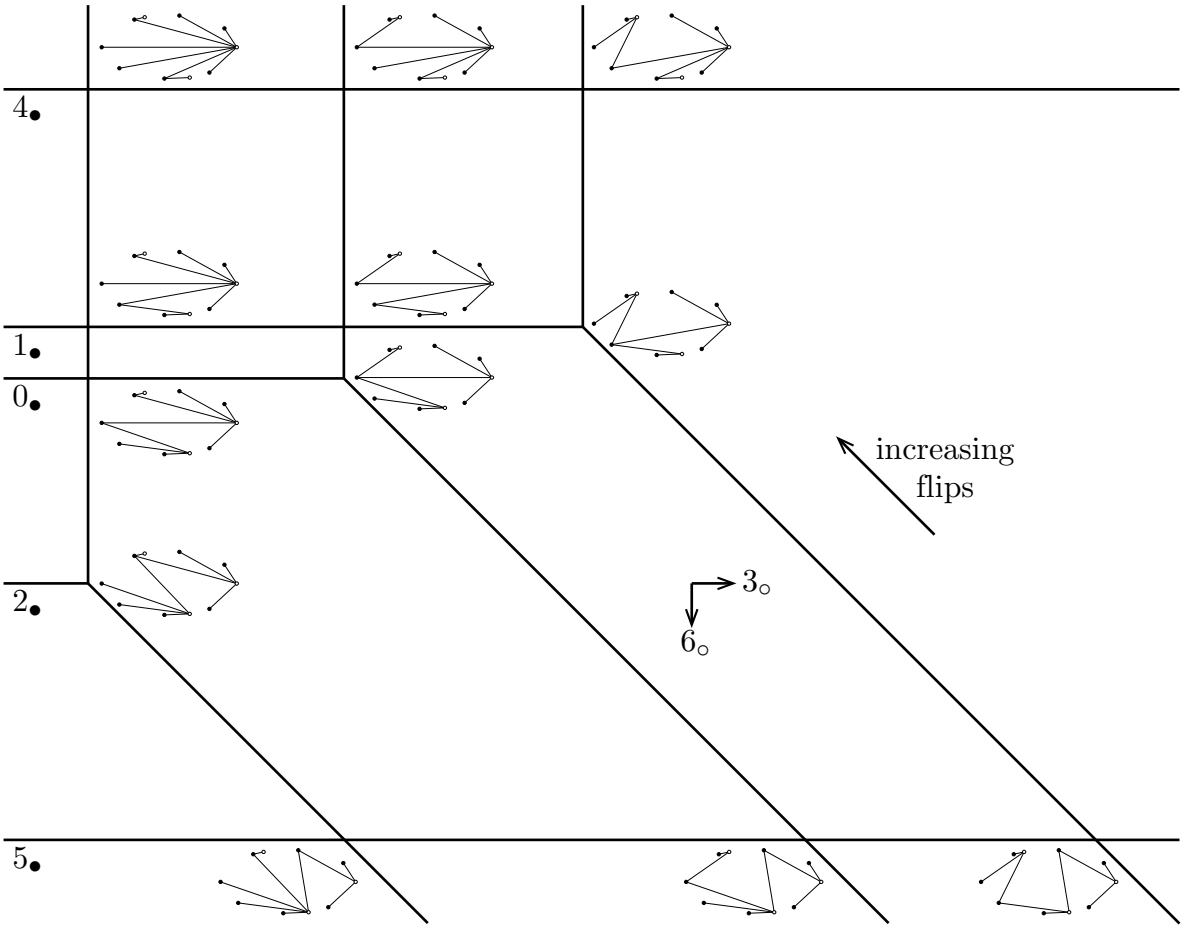


FIGURE 10. The tropical realization of the $(\varepsilon, I_\bullet, J_\circ)$-lattice. Here, $\varepsilon = -++-+--+$, $I_\bullet = [\![8_\bullet]\!] \smallsetminus \{3_\bullet, 6_\bullet\}$ and $J_\circ = \{3_\circ, 6_\circ, 9_\circ\}$. Compare to Figures 7 and 9. Note that $H_{4_\bullet}$ and $H_{5_\bullet}$ are degenerate tropical hyperplanes and that $H_{7_\bullet}$ is at infinity.

We have computed some coordinates of $(\varepsilon, I_\bullet, J_\circ)$-trees in Figure 11. For example,

$$g(\mathsf{t}_{\min})_{3_\circ} = -h(2_\bullet, 6_\circ) + h(5_\bullet, 6_\circ) - h(5_\bullet, 9_\circ) = -1,$$
$$\text{and} \qquad g(\mathsf{t}_{\min})_{6_\circ} = h(5_\bullet, 6_\circ) - h(5_\bullet, 9_\circ) = \sqrt{3} - 1.$$

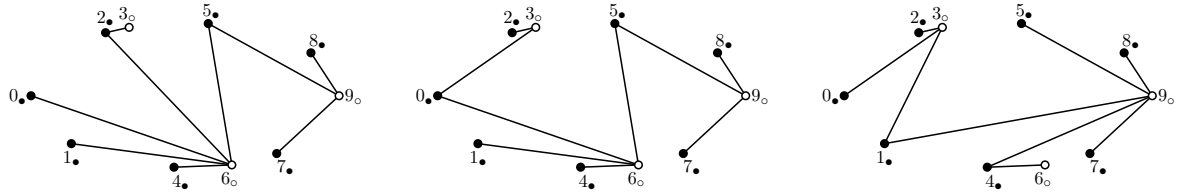


$g(\mathsf{t}_{\min})_{3_\circ} = -1$
$g(\mathsf{t}_{\min})_{6_\circ} = \sqrt{3} - 1$

$g(\mathsf{t})_{3_\circ} = \sqrt{3} - \sqrt{2}$
$g(\mathsf{t})_{6_\circ} = \sqrt{3} - 1$

$g(\mathsf{t}_{\max})_{3_\circ} = \sqrt{2} - \sqrt{3}$
$g(\mathsf{t}_{\max})_{6_\circ} = -\sqrt{2}$

FIGURE 11. Examples of computation of coordinates.

To conclude, let us gather all geometric realizations of the $(\varepsilon, I_\bullet, J_\circ)$-lattice encountered in this paper (see Corollaries 25, 31 and 32, and Theorem 36).

**Theorem 39.** *The increasing flip graph on $(\varepsilon, I_\bullet, J_\circ)$-trees can be realized geometrically as:*

*(1) the dual of the collection of cones of the $\varepsilon$-Cambrian fan of [RS09], or of normal cones of the $\varepsilon$-associahedron of [HL07], corresponding to an interval of the $\varepsilon$-Cambrian lattice,*
*(2) the dual of a flag regular triangulation of the subpolytope $\mathrm{U}_{I_\bullet, J_\circ}$ of a product of simplices,*
*(3) the dual of a coherent fine mixed subdivision of a generalized permutahedron,*
*(4) the edge graph of a polyhedral complex defined by a tropical hyperplane arrangement.*

## Acknowledgements

I am grateful to C. Ceballos, A. Padrol and C. Sarmiento for relevant comments and suggestions on the content of this paper. I also thank two anonymous referees for many relevant comments and suggestions concerning the presentation.

## References

[BB09] Olivier Bernardi and Nicolas Bonichon. Intervals in Catalan lattices and realizers of triangulations. *J. Combin. Theory Ser. A*, 116(1):55–75, 2009.
[BCP18] Nantel Bergeron, Cesar Ceballos, and Vincent Pilaud. Hopf dreams. Preprint, arXiv:1807.03044, 2018.
[Ber13] François Bergeron. Multivariate diagonal coinvariant spaces for complex reflection groups. *Adv. Math.*, 239:97–108, 2013.
[BM18] Emily Barnard and Thomas McConville. Lattices from graph associahedra and subalgebras of the Malvenuto-Reutenauer algebra. Preprint, arXiv:1808.05670, 2018.
[BMFPR11] Mireille Bousquet-Mélou, Éric Fusy, and Louis-François Préville-Ratelle. The number of intervals in the $m$-Tamari lattices. *Electron. J. Combin.*, 18(2):Paper 31, 26, 2011.
[BPR12] François Bergeron and Louis-François Préville-Ratelle. Higher trivariate diagonal harmonics via generalized Tamari posets. *Journal of Combinatorics*, 3(3):317–341, 2012.
[Cha07] F. Chapoton. Sur le nombre d'intervalles dans les treillis de Tamari. *Sém. Lothar. Combin.*, 55:Art. B55f, 18, 2005/07.
[CP17] Grégory Chatel and Vincent Pilaud. Cambrian Hopf Algebras. *Adv. Math.*, 311:598–633, 2017.
[CPS18] Cesar Ceballos, Arnau Padrol, and Camilo Sarmiento. Geometry of $\nu$-Tamari lattices in types $A$ and $B$. *Trans. Amer. Math. Soc.*, 2018.
[DRS10] Jesus A. De Loera, Jörg Rambau, and Francisco Santos. *Triangulations: Structures for Algorithms and Applications*, volume 25 of *Algorithms and Computation in Mathematics*. Springer Verlag, 2010.
[DS04] Mike Develin and Bernd Sturmfels. Tropical convexity. *Doc. Math.*, 9:1–27, 2004.
[FPR17] Wenjie Fang and Louis-François Préville-Ratelle. The enumeration of generalized Tamari intervals. *European J. Combin.*, 61:69–84, 2017.
[FZ02] Sergey Fomin and Andrei Zelevinsky. Cluster algebras. I. Foundations. *J. Amer. Math. Soc.*, 15(2):497–529, 2002.
[FZ03] Sergey Fomin and Andrei Zelevinsky. Cluster algebras. II. Finite type classification. *Invent. Math.*, 154(1):63–121, 2003.
[HL07] Christophe Hohlweg and Carsten Lange. Realizations of the associahedron and cyclohedron. *Discrete Comput. Geom.*, 37(4):517–543, 2007.
[HLT11] Christophe Hohlweg, Carsten Lange, and Hugh Thomas. Permutahedra and generalized associahedra. *Adv. Math.*, 226(1):608–640, 2011.
[HRS00] Birkett Huber, Jörg Rambau, and Francisco Santos. The Cayley trick, lifting subdivisions and the Bohne-Dress theorem on zonotopal tilings. *J. Eur. Math. Soc. (JEMS)*, 2(2):179–198, 2000.
[LP18] Carsten Lange and Vincent Pilaud. Associahedra via spines. *Combinatorica*, 38(2):443–486, 2018.
[LR98] Jean-Louis Loday and María O. Ronco. Hopf algebra of the planar binary trees. *Adv. Math.*, 139(2):293–309, 1998.
[MHPS12] Folkert Müller-Hoissen, Jean Marcel Pallo, and Jim Stasheff, editors. *Associahedra, Tamari Lattices and Related Structures. Tamari Memorial Festschrift*, volume 299 of *Progress in Mathematics*. Springer, New York, 2012.
[MR95] Claudia Malvenuto and Christophe Reutenauer. Duality between quasi-symmetric functions and the Solomon descent algebra. *J. Algebra*, 177(3):967–982, 1995.
[Pos09] Alexander Postnikov. Permutohedra, associahedra, and beyond. *Int. Math. Res. Not. IMRN*, (6):1026–1106, 2009.
[PP18] Vincent Pilaud and Viviane Pons. Permutrees. *Algebraic Combinatorics*, 1(2):173–224, 2018.
[PRV17] Louis-François Préville-Ratelle and Xavier Viennot. The enumeration of generalized tamari intervals. *Trans. Amer. Math. Soc.*, 369(7):5219–5239, 2017.

[PRW08] Alexander Postnikov, Victor Reiner, and Lauren K. Williams. Faces of generalized permutohedra. *Doc. Math.*, 13:207–273, 2008.
[Rea04] Nathan Reading. Lattice congruences of the weak order. *Order*, 21(4):315–344, 2004.
[Rea06] Nathan Reading. Cambrian lattices. *Adv. Math.*, 205(2):313–353, 2006.
[Rea16a] N. Reading. Finite Coxeter groups and the weak order. In *Lattice theory: special topics and applications. Vol. 2*, pages 489–561. Birkhäuser/Springer, Cham, 2016.
[Rea16b] N. Reading. Lattice theory of the poset of regions. In *Lattice theory: special topics and applications. Vol. 2*, pages 399–487. Birkhäuser/Springer, Cham, 2016.
[RS09] Nathan Reading and David E. Speyer. Cambrian fans. *J. Eur. Math. Soc.*, 11(2):407–447, 2009.
[Tam51] Dov Tamari. *Monoides préordonnés et chaînes de Malcev*. PhD thesis, Université Paris Sorbonne, 1951.

CNRS & LIX, École Polytechnique, Palaiseau
*E-mail address*: vincent.pilaud@lix.polytechnique.fr
*URL*: http://www.lix.polytechnique.fr/~pilaud/